

1 **Light into the darkness: Unifying the known and** 2 **unknown coding sequence space in microbiome** 3 **analyses**

4
5 Chiara Vanni^{1,2}, Matthew S. Schechter^{1,3}, Silvia G. Acinas⁴, Albert Barberán⁵, Pier Luigi
6 Buttigieg⁶, Emilio O. Casamayor⁷, Tom O. Delmont⁸, Carlos M. Duarte⁹, A. Murat Eren^{3,10},
7 Robert D. Finn¹¹, Renzo Kottmann¹, Alex Mitchell¹¹, Pablo Sanchez⁴, Kimmo Siren¹², Martin
8 Steinegger^{13,14}, Frank Oliver Glöckner^{15,16,2}, Antonio Fernandez-Guerra^{1,17*}

10 **Affiliations**

11 1 Microbial Genomics and Bioinformatics Research Group, Max Planck Institute for Marine
12 Microbiology, Celsiusstraße 1, 28359, Bremen, Germany
13 2 Jacobs University Bremen, Campus Ring 1, 28759 Bremen, Germany
14 3 Department of Medicine, University of Chicago, Chicago, IL 60637, USA
15 4 Department of Marine Biology and Oceanography, Institut de Ciències del Mar, CSIC,
16 Barcelona, Spain.
17 5 Department of Environmental Science, University of Arizona, Tucson, 85721 AZ, USA
18 6 Alfred Wegener Institute, Helmholtz Centre for Polar and Marine Research, Am Handelshafen
19 12, 27570 Bremerhaven, Germany
20 7 Center for Advanced Studies of Blanes CEAB-CSIC, Spanish Council for Research, Blanes,
21 Spain
22 8 Génomique Métabolique, Genoscope, Institut François Jacob, CEA, CNRS, Univ Evry,
23 Université Paris-Saclay, 91057 Evry, France
24 9 Red Sea Research Centre (RSRC) and Computational Bioscience Research Center (CBRC),
25 King Abdullah University of Science and Technology, Thuwal 23955, Saudi Arabia
26 10 Josephine Bay Paul Center, Marine Biological Laboratory, Woods Hole, MA 02543, USA
27 11 European Molecular Biology Laboratory, European Bioinformatics Institute (EMBL-EBI),
28 Wellcome Genome Campus, Hinxton, Cambridge CB10 1SD, UK
29 12 Section for Evolutionary Genomics, The GLOBE Institute, University of Copenhagen,
30 Copenhagen, Denmark
31 13 School of Biological Sciences, Seoul National University, Seoul, 08826, South Korea
32 14 Institute of Molecular Biology and Genetics, Seoul National University, Seoul, 08826, South
33 Korea
34 15 University of Bremen, MARUM, Leobener Str. 8, 28359 Bremen, Germany
35 Life Sciences and Chemistry, Campus Ring 1, 28759 Bremen, Germany
36 16 Computing Center, Helmholtz Center for Polar and Marine Research, Am Handelshafen 12,
37 27570 Bremerhaven, Germany

38 17 Lundbeck GeoGenetics Centre, The Globe Institute, University of Copenhagen, 1350
39 Copenhagen, Denmark

40

41 *Corresponding author: Antonio Fernandez-Guerra, antonio.fernandez-guerra@sund.ku.dk

42

43 Abstract

44 Bridging the gap between the known and the unknown coding sequence space is one of the
45 biggest challenges in molecular biology today. This challenge is especially extreme in microbiome
46 analyses where between 40% and 60% of the coding sequences detected are of unknown
47 function, and ignoring this fraction limits our understanding of microbial systems. Discarding the
48 uncharacterized fraction is not an option anymore. Here, we present an in-depth exploration of
49 the microbial unknown fraction through the lenses of a conceptual framework and a computational
50 workflow we developed to unify the microbial known and unknown coding sequence space. Our
51 approach partitions the coding sequence space in gene clusters and contextualizes them with
52 genomic and environmental information. We analyzed 415,971,742 genes predicted from 1,749
53 metagenomes and 28,941 bacterial and archaeal genomes, putting into perspective the extent of
54 the unknown fraction, its diversity, and its relevance in a genomic and environmental context.
55 With the identification of a target gene of unknown function for antibiotic resistance, we
56 demonstrate how a contextualized unknown coding sequence space provides a robust framework
57 for the generation of hypotheses that can be used to augment experimental data.

58 Introduction

59 Thousands of isolate, single-cell, and metagenome-assembled genomes are guiding us towards
60 a better understanding of how microbes shape life on Earth¹⁻⁷, thus bringing about a golden age
61 of microbial genomics. An ever-increasing number of genomes and metagenomes are unlocking
62 uncharted regions of microbial diversity^{1,8,9}, providing new perspectives on the evolution of life^{10,11}.
63 However, our rapidly growing inventories of new genes have a glaring issue: between 40% and
64 60% cannot be assigned to a known function¹²⁻¹⁵. Current analytical approaches for genomic and
65 metagenomic data¹⁶⁻²⁰ generally do not include this uncharacterized fraction in downstream
66 analyses, constraining their results to conserved pathways and housekeeping functions¹⁷. This
67 inability to handle shades of the unknown is an immense impediment to realizing the potential for
68 discovery of microbial genomics and microbiology at large^{12,21}.

69 Predicting function from traditional single sequence similarity appears to have yielded all it can²²⁻
70 ²⁴, thus several groups have attempted to resolve gene function by other means. Such efforts
71 include combining biochemistry and crystallography²⁵; using environmental co-occurrence²⁶; by
72 grouping those genes into evolutionarily related families²⁷⁻³⁰; using remote homologies^{31,32}; or
73 more recently using deep learning approaches^{33,34}. In 2018, Price et al.¹³ developed a high-
74 throughput experimental pipeline that provides mutant phenotypes for thousands of bacterial

75 genes of unknown function being one of the most promising methods to tackle the unknown.
76 Despite their promise, experimental methods are labor-intensive and require novel computational
77 methods that could bridge the existing gap between the known and unknown coding sequence
78 space (CDS-space).

79 Here we present a conceptual framework and a computational workflow that closes the gap
80 between the known and unknown CDS-space by connecting genomic and metagenomic gene
81 clusters. Our approach adds context to vast amounts of unknown biology, providing an invaluable
82 resource to get a better understanding of the unknown functional fraction and boost the current
83 methods for its experimental characterization. The application of our approach to 415,971,742
84 genes predicted from 1,749 metagenomes and 28,941 bacterial and archaeal genomes shows
85 that (1) the extent of the unknown fraction is smaller than expected, (2) that the diversity of gene
86 clusters in the unknown fraction is higher than in the known fraction, and (3) that the unknown
87 fraction is phylogenetically more conserved and is predominantly lineage-specific at the species
88 level. Finally, we show how we can connect all the outputs produced by our approach to augment
89 the results from experimental data and add context to genes of unknown function through
90 hypothesis-driven molecular investigations.

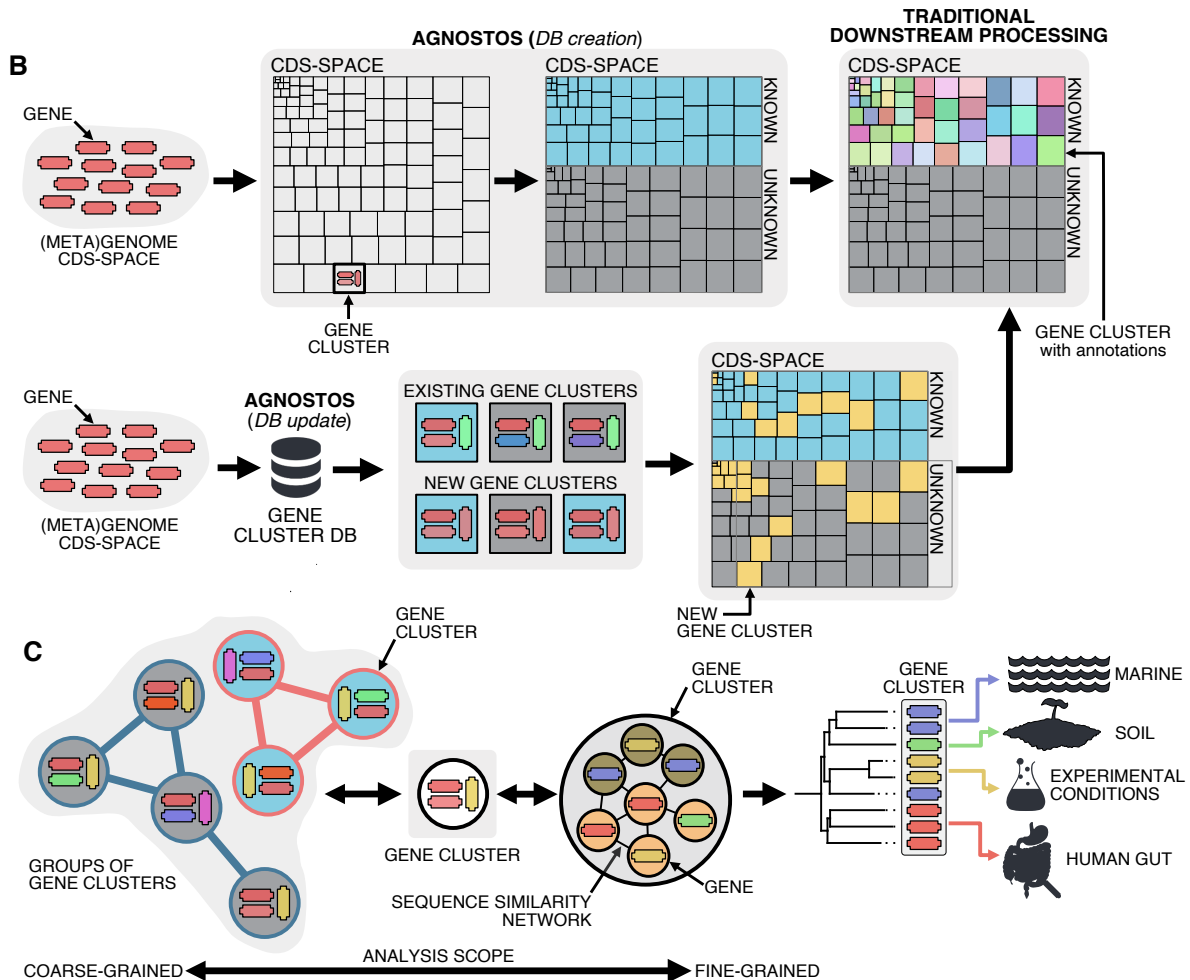
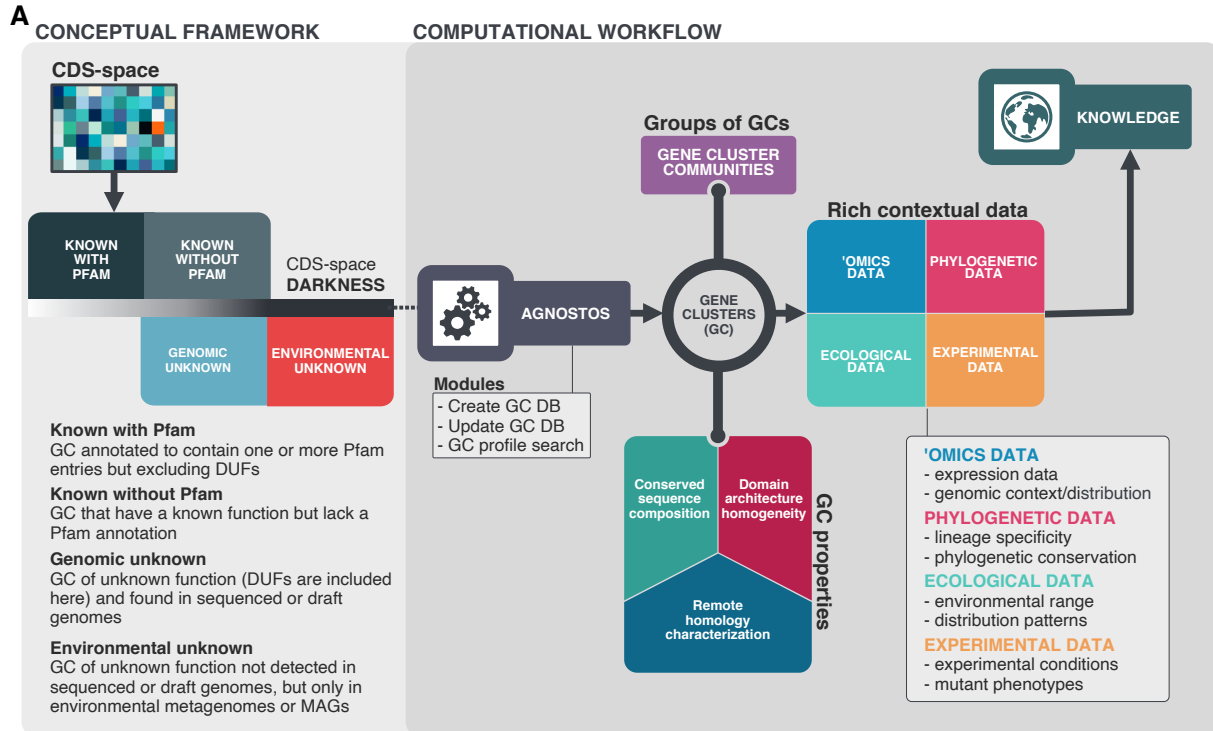
91

92 Results

93 A conceptual framework and a computational workflow to unify 94 the known and the unknown microbial coding sequence space

95 We created the conceptual and technical foundations to unify the known and unknown CDS-
96 space and provide a practical solution to one of the most significant ongoing challenges in
97 microbiome analyses. First, we conceptually partitioned the known and unknown fractions into (1)
98 Known with Pfam annotations (K), (2) Known without Pfam annotations (KWP), (3) Genomic
99 unknown (GU), and (4) Environmental unknown (EU) (Fig. 1A). The framework introduces a
100 subtle change of paradigm compared to traditional approaches where our objective is to provide
101 the best representation of the unknown space. We gear all our efforts towards finding sequences
102 without any evidence of known homologies by pushing the search space beyond the *twilight zone*
103 of sequence similarity³⁵. With this objective in mind, we use gene clusters (GCs) instead of genes
104 as the fundamental unit to compartmentalize the CDS-space owing to their unique characteristics
105 (Fig. 1B). GCs produce a structured CDS-space reducing its complexity (Fig. 1B), are
106 independent of the known and unknown fraction, are conserved across environments and
107 organisms, and can be used to aggregate information from different sources (Fig. 1A). Moreover,
108 the GCs provide a good compromise in terms of resolution for analytical purposes, and owing to
109 their unique properties, one can perform analyses at different scales. For fine-grained analyses,
110 we can exploit the gene associations within each GC; and for coarse-grained analyses, we can
111 create groups of GCs based on their shared homologies (Fig. 1B).

112



114 **Figure 1:** Conceptual framework to unify the known and unknown CDS-space and integration of the
115 framework in the current analytical workflows (A) Link between the conceptual framework and the
116 computational workflow to partition the CDS-space in the four conceptual categories. AGNOSTOS infers,
117 validates and refines the GCs and combines them in gene cluster communities (GCCs). Then, it classifies
118 them in one of the four conceptual categories based on their level of 'darkness'. Finally, we add context to
119 each GC based on several sources of information, providing a robust framework for the generation of
120 hypotheses that can be used to augment experimental data. (B) The computational workflow provides two
121 mechanisms to structure the CDS-space using GCs, de novo creation of the GCs (*DB creation*), or
122 integration of the dataset in an existing GC database (*DB update*). The structured CDS-space can then be
123 plugged into traditional analytical workflows to annotate the genes within each GC of the known fraction.
124 With AGNOSTOS, we provide the opportunity to easily integrate the unknown fraction into the current
125 microbiome analyses. C) The versatility of the GCs enables analyses at different scales depending on the
126 scope of our experiments. We can group GCs in gene cluster communities based on their shared
127 homologies to perform coarse-grained analyses. On the other hand, we can design fine-grained analyses
128 using the relationships between the genes in a GC, i.e., detecting network modules in the GC inner
129 sequence similarity network. Additionally, the fact that GCs are conserved across environments, organisms
130 and experimental conditions gives us access to an unprecedented amount of information to design and
131 interpret experimental data.

132

133 Driven by the concepts defined in the conceptual framework, we developed AGNOSTOS, a
134 computational workflow that infers, validates, refines, and classifies GCs in the four proposed
135 categories (Fig. 1A; Fig. 1B; Supp. Fig 1). AGNOSTOS provides two operational modules (*DB*
136 *creation* and *DB update*) to produce GCs with a highly conserved intra-homogeneous structure
137 (Fig. 1B), both in terms of sequence similarity and domain architecture homogeneity; it exhausts
138 any existing homology to known genes and provides a proper delimitation of the unknown CDS-
139 space before classifying each GC in one of the four categories. In the last step, we decorate each
140 GC with a rich collection of contextual data that we compile from different sources, or that we
141 generate by analyzing the GC contents in different contexts (Fig. 1A). For each GC, we also offer
142 several products that can be used for analytical purposes like improved representative
143 sequences, consensus sequences, sequence profiles for MMseqs2³⁶ and HHblits³⁷, or the GC
144 members as a sequence similarity network (see Online Methods). To complement the collection,
145 we also provide a subset of what we define as *high-quality* GCs. The defining criteria are (1) the
146 representative is a complete gene and (2) more than one-third of genes within a GC are complete
147 genes.

148 Partitioning and contextualizing the coding sequence space of 149 genomes and metagenomes

150 We used our approach to explore the unknown CDS-space of 1,749 microbial metagenomes
151 derived from human and marine environments, and 28,941 genomes from GTDB_r86 (Supp Fig
152 2A).

153 The initial gene prediction of AGNOSTOS (Supp Fig 1) produced 322,248,552 genes from the
154 environmental dataset and assigned Pfam annotations to 44% of them. Next, it clustered the
155 predicted genes in 32,465,074 GCs. For the downstream processing, we kept 3,003,897 GCs
156 (83% of the original genes) after filtering out any GC that contained less than ten genes³⁸
157 removing 9,549,853 clusters and 19,911,324 singletons (Supp Fig 2A; Supp. Note 1). The
158 validation process selected 2,940,257 *good-quality* clusters (Fig. 1B; Supp. Table 1; Supp. Note
159 2), which resulted in 43% of them being members of the unknown CDS-space after the
160 classification and remote homology refinement steps (Supp Fig 2A, Supp. Note 3).

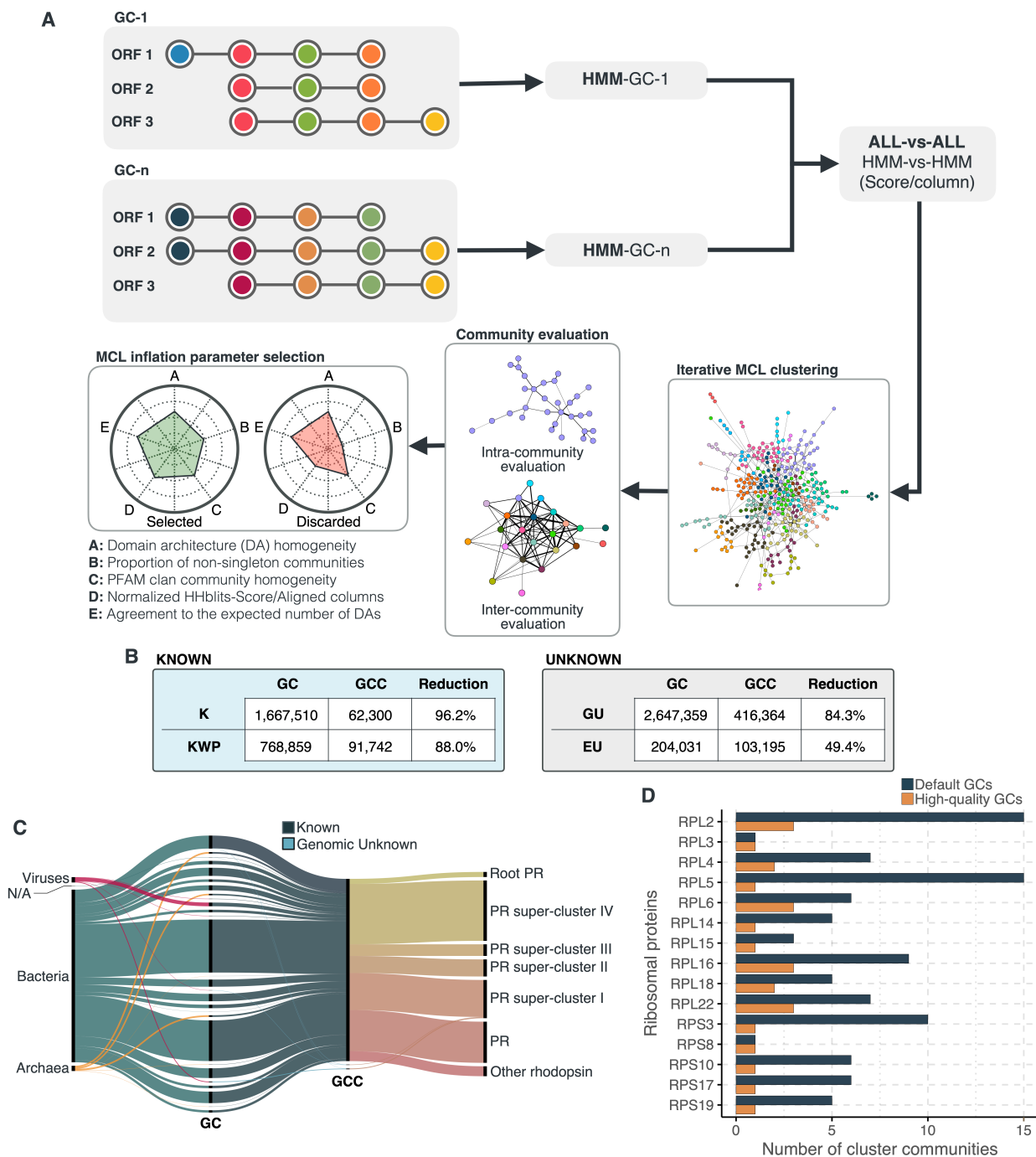
161 We build the link between the environmental and genomic CDS-space by expanding the final
162 collection of GCs with the genes predicted from GTDB_r86 (Supp Fig 2A). Our environmental
163 GCs already included 72% of the genes from GTDB_r86; 22% of them created 2,400,037 new
164 GCs, and the rest 6% resulted in singleton GCs (Supp Fig 2A; Supp. Note 4; Supp. Note 5). The
165 final dataset includes 5,287,759 GCs (Supp Fig 2A), with both datasets sharing only 922,599 GCs
166 (Supp Fig 2B). The addition of the GTDB_r86 genes increased the proportion of GCs in the
167 unknown CDS-space to 54%. As the final step, the workflow generated a subset of 203,217 *high-*
168 *quality* GCs (Supp Table 2; Supp Fig 3). In these *high-quality* clusters, we identified 12,313
169 clusters potentially encoding for small proteins (≤ 50 amino acids). Most of these GCs are
170 unknown (66% of them), which agrees with recent findings on novel small proteins from
171 metagenomes³⁹.

172 The KWP category contains the largest proportion of incomplete ORFs (Supp. Table 3), impeding
173 the detection and assignment of Pfam domains. But it also incorporates sequences with an
174 unusual amino acid composition that has homology to proteins with high levels of disorder in the
175 DPD database⁴⁰ and that have characteristic functions of the intrinsically disordered proteins⁴¹
176 (IDP) like cellular processes and signaling as predicted by eggNOG annotations (Supp. Table 4).
177 As part of the workflow, each GC is complemented with a rich set of information, as shown in Fig
178 1A (Supp. Table 5; Supp Note 6).

179 Beyond the twilight zone, communities of gene clusters

180 The method we developed to group GCs in gene cluster communities (GCCs) (Fig. 2A) reduced
181 the final collection of GCs by 87%, producing 673,601 GCCs (Fig. 2B; Supp. Note 7). We validated
182 the ability of our approach in capturing remote homologies between related GCs using two well-
183 known gene families present in our environmental datasets, proteorhodopsins⁴² and bacterial
184 ribosomal proteins⁴³. In our dataset, 64 GCs (12,184 genes) and 3 GCCs (Supp Note 8) contained
185 sequences classified as proteorhodopsin (PR). One *Known* GCC contained 99% of the PR
186 annotated genes (Fig. 2C), with the only exception of 85 genes taxonomically annotated as viral
187 and assigned to the *PR Supercluster I*⁴⁴ enclosed in two GU communities (five GU gene clusters;
188 Supp Note 8). For the ribosomal proteins, the results were not so satisfactory. We identified 1,843
189 GCs (781,579 genes) and 98 GCCs. The number of GCCs is larger compared to the expected
190 number of ribosomal proteins families (16) used for validation. When we use *high-quality* GCs
191 (Supp. Note 8), we get closer to the expected number of GCCs (Fig. 2D). With this subset, we
192 identified 26 GCCs and 145 GCs (1,687 genes). The cross-validation of our method against the
193 approach used in Méheust et al.⁴³ (Supp. Note 9) confirms the intrinsic complexity of analyzing
194 metagenomic data. Both approaches showed a high agreement in the GCCs identified (Supp.
195 Table 9-1). Still, our method inferred fewer GCCs for each of the ribosomal protein families
196 (Supplementary Figure 9-3), coping better with the nuisances of a metagenomic setup, like
197 incomplete genes (Supp. Table 6).

198



199
 200 **Figure 2:** Overview and validation of the workflow to aggregate GCs in communities. (A) We inferred a
 201 gene cluster homology network using the results of an all-vs-all HMM gene cluster comparison with
 202 HHBLITS. The edges of the network are based on the HHblits-score/Aligned-columns. Communities are
 203 identified by an iterative screening of different MCL inflation parameters and evaluated using five different
 204 metrics that take into account the inter- and intra-community properties. (B) Comparison of the number of
 205 GCs and GCCs for each of the functional categories. (C) Validation of the GCCs inference based on the
 206 environmental genes annotated as proteorhodopsins. Ribbons in the alluvial plot are genes, and each

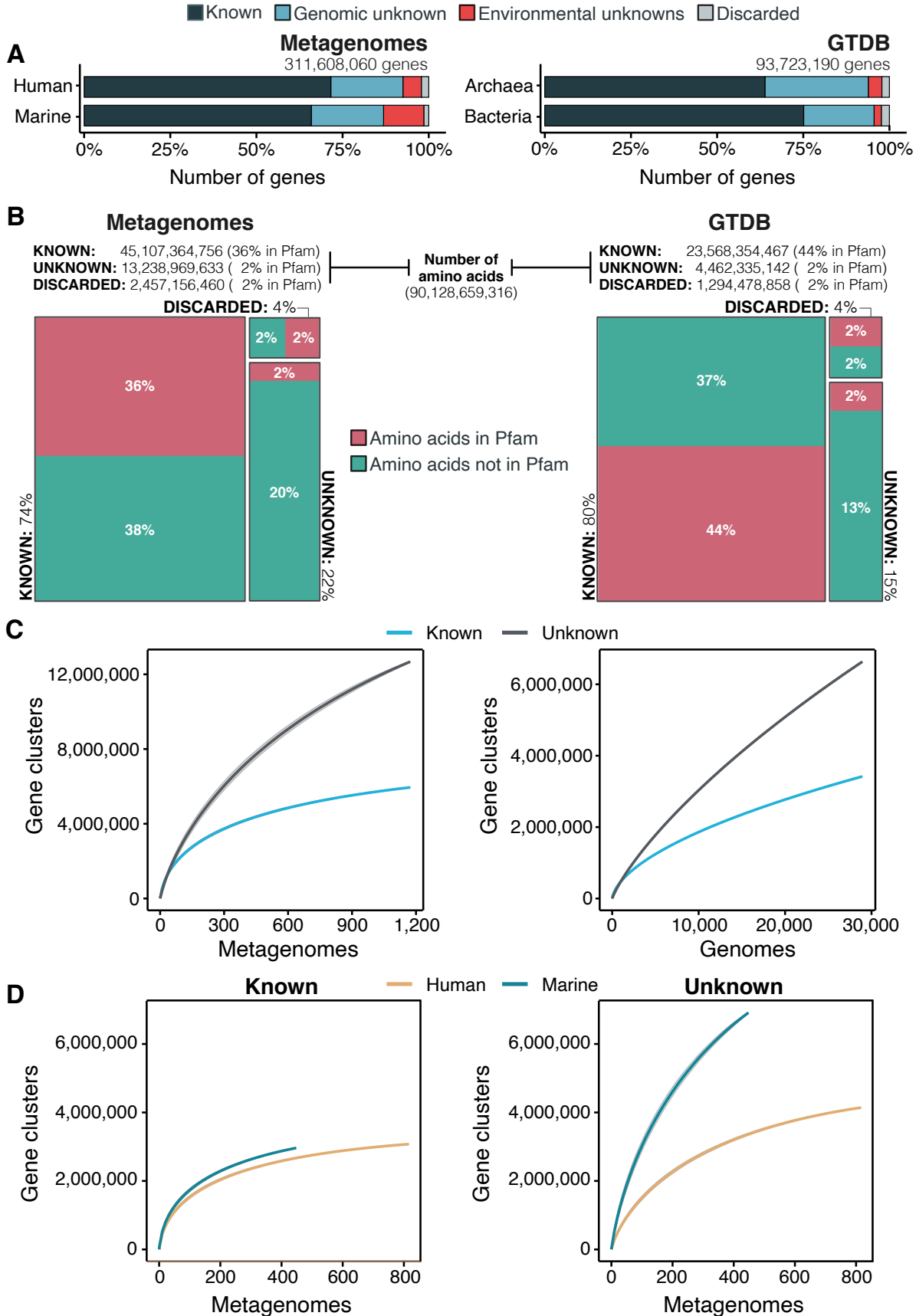
207 stacked bar corresponds (from left to right) to the (1) gene taxonomic classification at the domain level, (2)
208 GC membership, (3) GCC membership and (4) MicRhoDE operational classification. (D) Validation of the
209 GCCs inference based on ribosomal proteins based on standard and high-quality GCs.

210 **A smaller but highly diverse unknown coding sequence space**

211 Combining clustering and remote homology searches reduce the extent of the unknown CDS-
212 space compared to the traditional genomic and metagenomic analysis approaches (Fig. 3A). Our
213 workflow recruited as much as 71% of genes in human-related metagenomic samples and 65%
214 of the genes in marine metagenomes into the known CDS-space. In both human and marine
215 microbiomes, the genomic unknown fraction showed a similar proportion of genes (21%, Fig. 3A).
216 The number of genes corresponding to EU gene clusters is higher in marine metagenomes; in
217 total, 12% of the genes are part of this GC category. We obtained a comparable result when we
218 evaluated the genes from the GTDB_r86, 75% of bacterial and 64% of archaeal genes were part
219 of the known CDS-space. Archaeal genomes contained more unknowns than those from Bacteria,
220 where 30% of the genes are classified as genomic unknowns in Archaea, and only 20% in
221 Bacteria (Fig. 3A; Supp. Table 7). We observed a similar trend when we evaluated the number of
222 amino acids belonging to the known and unknown CDS-space. From the 90,128,659,316 amino
223 acids analyzed, the majority of the amino acids in metagenomes (74%) and in GTDB_r86 (80%)
224 are in the known CDS-space (Fig. 3B; Supp. Table 7). In both cases, approximately 40% of the
225 amino acids in the known CDS-space were part of a Pfam domain (Fig. 3B; Supp. Table 7). The
226 proportion of amino acids in the unknown CDS-space ranged from the 22% in metagenomes and
227 15% in GTDB_r86. In both cases, only 2% of the amino acids in the unknown CDS-space were
228 covered by a Pfam domain.

229 To evaluate the coverage of our dataset, we calculated the accumulation rates of GCs and GCCs.
230 For the metagenomic dataset we used 1,264 metagenomes (18,566,675 GCs and 282,580
231 GCCs) and for the genomic dataset 28,941 genomes (9,586,109 GCs and 496,930 GCCs). The
232 rate of accumulation of unknown GCs was three times higher than the known (2 times for the
233 genomic), and both cases were far from reaching a plateau (Fig. 3C). This is not the case for the
234 GCC accumulation curves (Supp Fig 4B), where they reached a plateau. The rate of accumulation
235 is largely determined by the number of singletons, and especially singletons from EUs (Supp note
236 11 and Supp Fig 5). While the accumulation rate of known GCs between marine and human
237 metagenomes is almost identical, there are striking differences for the unknown GCs (Fig. 3D).
238 These differences are maintained even when we remove the virus-enriched samples from the

239 marine metagenomes (Supp Fig 4A). Although the marine metagenomes include a large variety
240 of environments, from coastal to the deep sea, the known space remains quite constrained.
241 Despite only including marine and human metagenomes in our database, our coverage to other
242 databases and environments is quite comprehensive, with an overall coverage of 76% (Supp.
243 Note 12). The lowest covered biomes are freshwater, soil and human non-digestive as revealed
244 by the screening of MGnify¹⁶ (release 2018_09; 11 biomes; 843,535,6116 proteins) where we
245 assigned 74% of the MGnify proteins into one of our categories (Supplementary Fig. 6).
246



248 **Figure 3:** The extent of the known and unknown coding sequence space (A) Proportion of genes in the
249 known and unknown. (B) Amino acid distribution in the known and unknown CDS-space. (C) Accumulation
250 curves for the known and unknown CDS-space at the GC- level for the metagenomic and genomic data.
251 from TARA, MALASPINA, OSD2014 and HMP-I/II projects. (D) Collector curves comparing the human and
252 marine biomes. Colored lines represent the mean of 1000 permutations and shaded in grey the standard
253 deviation. Non-abundant singleton clusters were excluded from the accumulation curves calculation.

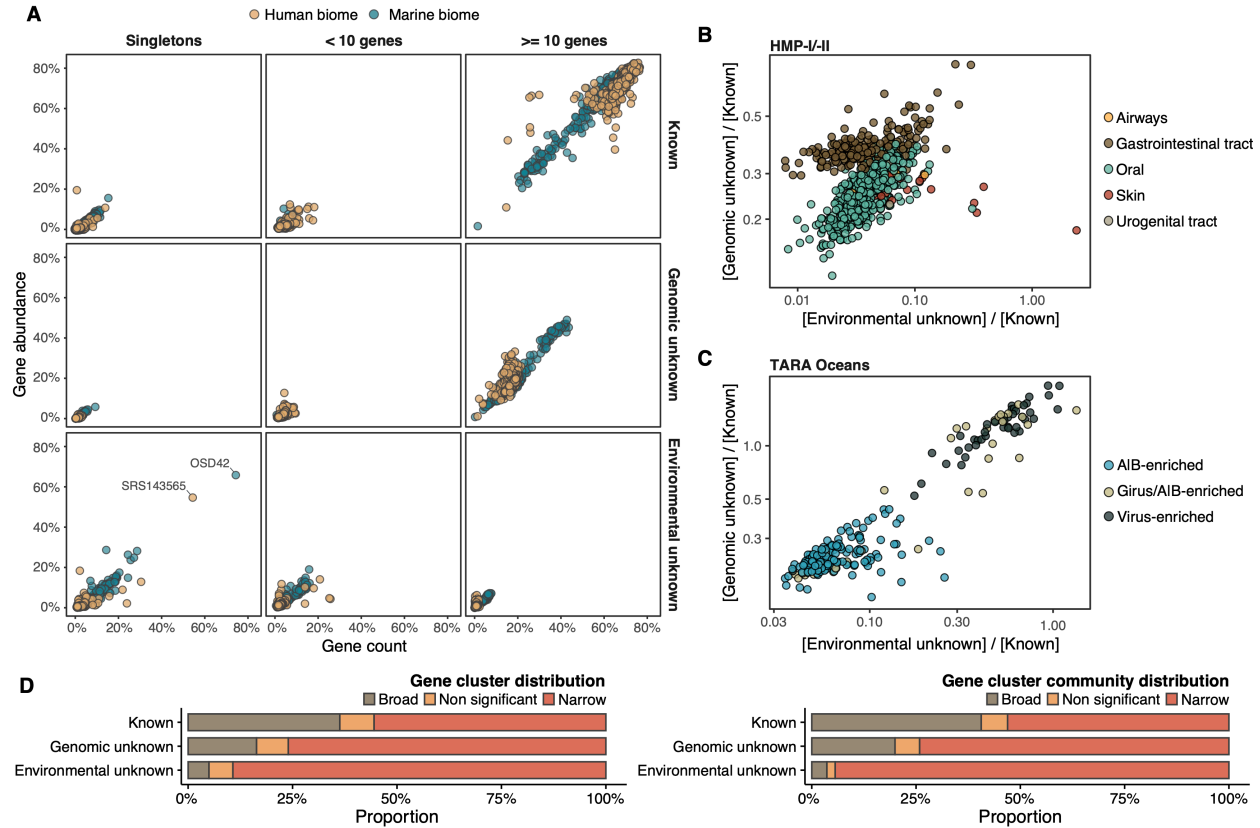
254 Revealing the importance of the unknown coding sequence space 255 in marine and human environments

256 Although the role of the unknown fraction in the environment is still a mystery, the large number
257 of gene counts and abundance observed underlines its inherent ecological relevance (Fig. 4A).
258 In some samples, the genomic unknown fraction can account for more than 40% of the total gene
259 abundance observed (Fig. 4A). The environmental unknown fraction is also relevant in several
260 samples, where singleton GCs are the majority (Fig. 4A). We identified two metagenomes with
261 an unusual composition in terms of environmental unknown singletons. The marine metagenome
262 corresponds to a sample from Lake Faro (OSD42), a meromictic saline with a unique extreme
263 environment where Archaea plays an important role⁴⁵. The HMP metagenome (SRS143565)
264 corresponds to a human sample from the right cubital fossa from a healthy female subject. To
265 understand the unusual composition of this metagenome, we should perform further analyses to
266 discard potential technical artifacts like sample contamination.

267 The ratio between the unknown and known GCs revealed that the metagenomes located at the
268 upper left quadrant in Fig. 4B-C are enriched in GCs of unknown function. In human
269 metagenomes, we can distinguish between body sites, with the gastrointestinal tract, where
270 microbial communities are expected to be more diverse and complex, especially enriched with
271 genomic unknowns. The HMP metagenomes with the largest ratio of unknowns are those
272 samples identified to contain crAssphages^{46,47} and HPV viruses⁴⁸ (Supp. Table 8; Supp. Fig. 7).
273 Consistently, in marine metagenomes (Fig. 4D) we can separate between size fractions, where
274 the highest ratio in genomic and environmental unknowns corresponds to the ones enriched with
275 viruses and giant viruses.

276 To complement the previous findings, we performed a large-scale analysis to investigate the GC
277 occurrence patterns in the environment. The narrow distribution of the unknown fraction (Fig. 4D)
278 suggests that these GCs might provide a selective advantage and be necessary for the adaptation
279 to specific environmental conditions. But the pool of broadly distributed environmental unknowns
280 is the most interesting result. We identified traces of potential ubiquitous organisms left

281 uncharacterized by traditional approaches, as more than 80% of these GCs cannot be associated
 282 with a metagenome-assembled genome (MAG) (Supp Table 9, Supp. Note 10).
 283



284

285 **Figure 4:** Distribution of the unknown coding sequence space in the human and marine metagenomes
 286 (A) Ratio between the proportion of the number of genes and their estimated abundances per cluster
 287 category and biome. Columns represented in the facet depicts three cluster categories based on the size
 288 of the clusters. (B) Relationship between the ratio of Genomic unknowns and Environmental unknowns in
 289 the HMP-I/II metagenomes. Gastrointestinal tract metagenomes are enriched in Genomic unknown
 290 coding sequences compared to the other body sites. (C) Relationship between the ratio of Genomic
 291 unknowns and Environmental unknowns in the TARA Oceans metagenomes. Girus and virus enriched
 292 metagenomes show a higher proportion of both unknown coding sequences (genomic and
 293 environmental) compared to the Archaea|Bacteria enriched fractions. (D) Environmental distribution of
 294 GCs and GCCs based on Levin's niche breadth index. We obtained the significance values after
 295 generating 100 null gene cluster abundance matrices using the quasiswap algorithm.
 296

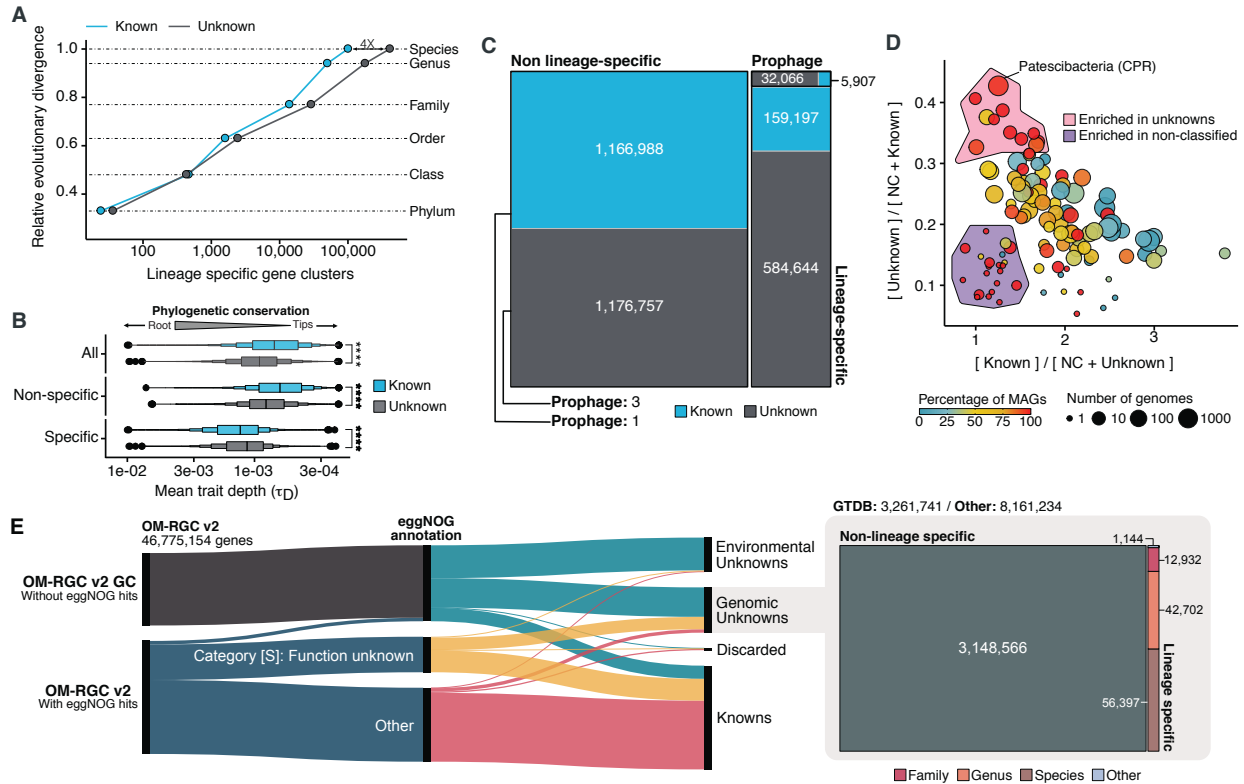
297 **The genomic unknown coding sequence space is lineage-specific**

298 We already showed that the unknown CDS-space is habitat-specific and might be relevant for
 299 organism adaptation. With the inclusion of the genomes from GTDB_r86, we have accessed a

300 phylogenomic framework to assess how conserved and exclusive is a GC within a lineage
301 (lineage-specificity⁴⁹) and the clade depth where organisms share a GC (phylogenetic
302 conservation⁵⁰). We identified 781,814 lineage-specific GCs and 464,923 phylogenetically
303 conserved ($P < 0.05$) GCs in Bacteria (Supp. Table 10; Supp. Note 13 for Archaea). The number
304 of lineage-specific GCs increases with the Relative Evolutionary Distance¹¹ (Fig. 5A) and
305 differences between the known and the unknown fraction start to be evident at the Family level.
306 The unknown GCs are more phylogenetically conserved than the known (Fig. 5B, $p < 0.0001$),
307 revealing the importance of the genome's uncharacterized fraction. However, this is not the case
308 for the lineage-specific and phylogenetically conserved GCs, where the unknown GCs are less
309 phylogenetically conserved (Fig. 5B), agreeing with the large number of lineage-specific GCs at
310 Genus and Species level. To discard the possibility that the lineage-specific GCs of unknown
311 function have a viral origin, we screened all GTDB_r86 genomes for prophages. We only found
312 37,163 lineage-specific GCs in prophage genomic regions, being 86% of them GCs of unknown
313 function. After unveiling the potential relevance of the GCs of unknown function in bacterial
314 genomes, we identified phyla in GTDB_r86 enriched with these types of clusters. A clear pattern
315 emerged when we partitioned the phyla based on the ratio of known to unknown GCs and vice
316 versa (Fig. 5D), the phyla with a larger number of MAGs are enriched in GCs of unknown function
317 Figure 5D. Phyla with a high proportion of non-classified GCs (those discarded during the
318 validation steps) contain a small number of genomes and are primarily composed of MAGs. These
319 groups of phyla highly enriched in unknowns and represented mainly by MAGs include newly
320 described phyla such as *Cand. Riflebacteria* and *Cand. Patescibacteria*^{9,51,52}, both with the largest
321 unknown to known ratio.

322 We demonstrate the possibility to bridge genomic and metagenomic data and simultaneously
323 unify the known and unknown CDS-space by integrating the new Ocean Microbial Reference
324 Gene Catalog⁵³ (OM-RGC v2) in our database. We assigned 26,170,875 genes to known GCs,
325 11,422,975 to genomic unknowns, 8,661,221 to environmental unknown and 520,083 were
326 discarded. From the 11,422,975 genes classified as genomic unknowns, we could associate
327 3,261,741 to a GTDB_r86 genome and we identified 113,175 as lineage-specific. The alluvial plot
328 in Fig. 5E depicts the new organization of the OM-RGC v2 after being integrated into our
329 framework, and how we can provide context to the two original types of unknowns in the OM-
330 RGC (those annotated as category S in eggNOG⁵⁴ and those without known homologs in the
331 eggNOG database⁵³) that can lead to potential experimental targets at the organism level to
332 complement the metatranscriptomic approach proposed by Salazar et al⁵³.

333



334

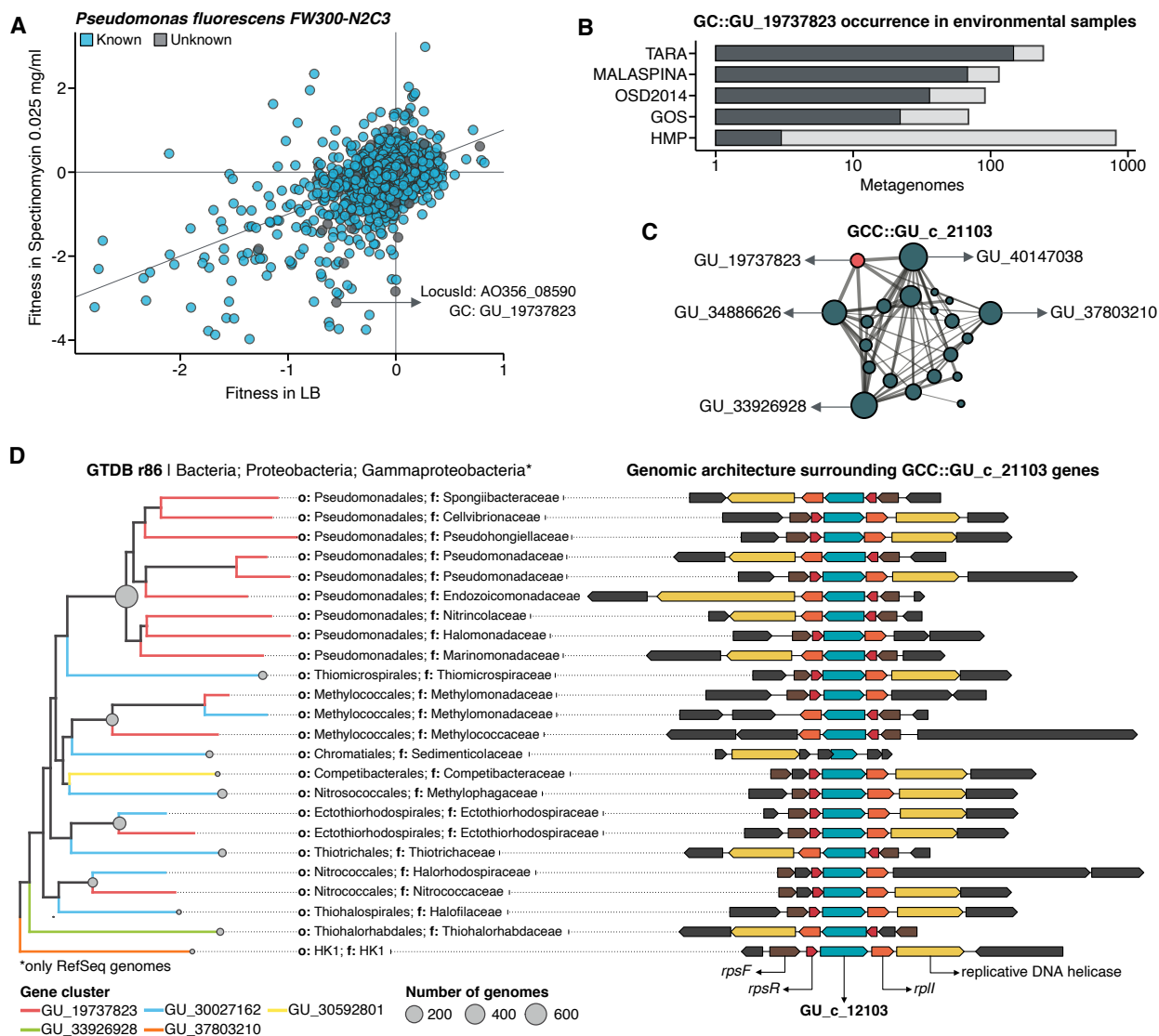
335 **Figure 5:** Phylogenomic exploration of the unknown coding sequence space. (A) Distribution of the
 336 lineage-specific GCs by taxonomic level. Lineage-specific unknown GCs are more abundant in the lower
 337 taxonomic levels (genus, species). (B) Phylogenetic conservation of the known and unknown coding
 338 sequence space in 27,372 bacterial genomes from GTDB_r86. We observe differences in the
 339 conservation between the known and the unknown coding sequence space for lineage- and non-lineage
 340 specific GCs (paired Wilcoxon rank-sum test; all p-values < 0.0001). (C) The majority of the lineage-
 341 specific clusters are part of the unknown coding sequence space, being a small proportion found in
 342 prophages present in the GTDB_r86 genomes. (D) Known and unknown coding sequence space of the
 343 27,732 GTDB_r86 bacterial genomes grouped by bacterial phyla. Phyla are partitioned based on the ratio
 344 of known to unknown GCs and vice versa. Phyla enriched in MAGs have higher proportions in GCs of
 345 unknown function. Phyla with a high proportion of non-classified clusters (NC; discarded during the
 346 validation steps) tend to contain a small number of genomes. (E) The left side of the alluvial plot shows
 347 the uncharacterized (OM-RGC v2 GC) and characterized (OM-RGC v2) fraction of the gene catalog. The
 348 functional annotation is based on the eggNOG annotations provided by Salazar et al.⁵³. The right side of
 349 the alluvial plot shows the new organization of the OM-RGC v2 coding sequence space based on the
 350 approach described in this study. The treemap in the right links the metagenomic and genomic space
 351 adding context to the unknown fraction of the OM-RGC v2

352

353 Augmenting experimental data through a structured coding 354 sequence space

355 We selected one of the experimental conditions tested in Price et al.¹³ to demonstrate the potential
356 of our approach to augment experimental data. We compared the fitness values in plain rich
357 medium with added Spectinomycin dihydrochloride pentahydrate to the fitness in plain rich
358 medium (LB) in *Pseudomonas fluorescens* FW300-N2C3 (Fig. 6A). This antibiotic inhibits protein
359 synthesis and elongation by binding to the bacterial 30S ribosomal subunit and interferes with the
360 peptidyl tRNA translocation. We identified the gene with locus id AO356_08590 that presents a
361 strong phenotype (fitness = -3.1; t = -9.1) and has no known function. This gene belongs to the
362 genomic unknown GC GU_19737823. We can track this GC into the environment and explore
363 the occurrence in the different samples we have in our database. As expected, the GC is mostly
364 found in non-human metagenomes (Fig. 6B) as *Pseudomonas* are common inhabitants of soil
365 and water environments⁵⁵. However, finding this GC also in human-related samples is very
366 interesting, due to the potential association of *P. fluorescens* and human disease where Crohn's
367 disease patients develop serum antibodies to this microbe⁵⁶. We can add another layer of
368 information to the selected GC by looking at the associated remote homologs in the GCC
369 GU_c_21103 (Fig. 6C). We identified all the genes in the GTDB_r86 genomes that belong to the
370 GCC GU_c_21103 (Supp. Table 11) and explored their genomic neighborhoods. All members
371 from GU_c_21103 are constrained to the class *Gammaproteobacteria*, and interestingly
372 GU_19737823 is mostly exclusive to the order *Pseudomonadales*. The gene order in the different
373 genomes analyzed is highly conserved, finding GU_19737823 after the *rpsF::rpsR* operon and
374 before *rplI*. *rpsF* and *rpsR* encode for 30S ribosomal proteins, the prime target of spectinomycin.
375 The combination of the experimental evidence and the associated data inferred by our approach
376 provides strong support to generate the hypothesis that the gene AO356_08590 might be involved
377 in the resistance to spectinomycin.

378



379

380 **Figure 6:** Augmenting experimental data with GCs of unknown function. (A) We used the fitness values
 381 from the experiments from Price et al.¹³ to identify genes of unknown function that are important for fitness
 382 under certain experimental conditions. The selected gene belongs to the genomic unknown GC
 383 GU_19737823 and presents a strong phenotype (fitness = -3.1; $t = -9.1$) (B) Occurrence of GU_19737823
 384 in the metagenomes used in this study. Darker bars depict the number of metagenomes where the GC is
 385 found. (C) GU_19737823 is a member of the GCC GU_c_21103. The network shows the relationships
 386 between the different GCs members of the gene cluster community GU_c_21103. The size of the node
 387 corresponds to the node degree of each GC. Edge thickness corresponds to the bitscore/column metric.
 388 Highlighted in red is GU_19737823. (D) We identified all the genes in the GTDB_r86 genomes that belong
 389 to the GCC GU_c_21103 and explored their genomic neighborhoods. GU_c_21103 members were
 390 constrained to the class Gammaproteobacteria, and GU_19737823 is mostly exclusive to the order
 391 Pseudomonadales. The gene order in the different genomes analyzed is highly conserved, finding
 392 GU_19737823 after the *rpsF*::*rpsR* operon and before *rplI*. *rpsF* and *rpsR* encode for the 30S ribosomal
 393 protein S6 and 30S ribosomal protein S18 respectively. The GTDB_r86 subtree only shows RefSeq
 394 genomes. Branch colors correspond to the different GCs found in GU_c_21103. Bubble plot depicts the
 395 number of genomes with a gene that belongs to GU_c_21103.

396 Discussion

397 We present a new conceptual framework and computational workflow to unify the known and
398 unknown CDS-space in microbial analyses. Using this framework, we performed an in-depth
399 exploration of the microbial unknown CDS-space. We demonstrated that we could link the
400 unknown fraction of metagenomic studies to specific genomes and provide a powerful tool for
401 hypothesis generation. During the last years, the microbiome community has established a
402 standard operating procedure¹⁷ for analyzing metagenomes that we can briefly summarize into
403 (1) assembly, (2) gene prediction, (3) gene catalog inference, (4) binning, and (5) characterization.
404 Thanks to recent computational developments^{36,57}, we envisioned an alternative to this workflow
405 where we can maximize the information used when analyzing genomic and metagenomic data.
406 In addition, we provide a mechanism to reconcile top-down and bottom-up approaches, thanks to
407 the well-structured CDS-space proposed by our framework. AGNOSTOS can create
408 environmental- and organism-specific variations of a seed GC database. Then, it integrates the
409 predicted genes from new genomes and metagenomes and dynamically creates and classifies
410 new GCs with those genes not integrated during the initial step (Fig. 1B). Afterward, the potential
411 functions of the known GCs can be carefully characterized by incorporating them into the
412 traditional workflows.

413 One of the most appealing characteristics of our approach is that the GCs provide unified groups
414 of homologous genes across environments and organisms indifferently if they belong to the
415 known or unknown CDS-space, and we can contextualize the unknown fraction using this
416 genomic and environmental information. Our combination of partitioning and contextualization
417 features a smaller unknown CDS-space than we expected. On average, for our genomic and
418 metagenomic data, only 30% of the genes fall in the unknown fraction. One hypothesis to
419 reconcile this surprising finding is that until recently, the methodologies to identify remotely
420 homologous sequences in large datasets were computationally prohibitive. New methods^{36,37}, like
421 the ones used in AGNOSTOS, are enabling large scale distant homology searches. Still, one has
422 to apply conservative measures to control the trade-off between specificity and sensitivity to avoid
423 overclassification.

424 We found that the majority of the coding sequence space at gene and amino acid is known, both
425 in genomes and metagenomes. However, it presents a high diversity as shown in the GC
426 accumulation curves highlighting the vast remaining untapped microbial fraction and its potential
427 importance for niche adaptation owing to its narrow ecological distribution. In a genomic context,
428 the unknown fraction is predominantly species' lineage-specific and phylogenetically more

429 conserved than the known fraction, supporting the signal observed in the environmental data and
430 emphasizing that the unknown fraction should not be ignored. We also ruled out the effect of
431 prophages, strengthening the hypothesis that the lineage-specific GCs of unknown function might
432 be associated with the mechanisms of microbial diversification and niche adaptation as a result
433 of the constant diversification of gene families and the survival of new gene lineages^{58,59}. It is
434 worth noting that we need to explore further the unknown fraction to identify new potential protein
435 domains. Only 10% of the unknown CDS-space amino acids are part of a Pfam domain (DUF and
436 others); this contrasts with the numbers observed in the known CDS-space, where Pfam domains
437 include 50% of the amino acids.

438 Metagenome-assembled genomes are not only unveiling new regions of the microbial universe
439 (42% of the genomes in GTDB_r86), but they are also enriching genes of unknown function in
440 the tree of life. We investigated the unknown CDS-space of *Cand.* Patescibacteria, more
441 commonly known as Candidate Phyla Radiation (CPR), a phylum that has raised considerable
442 interest due to their unusual biology⁹. We provide a collection of 54,343 lineage-specific GCs of
443 unknown function at different taxonomic level resolutions (Supp. Table 12; Supp. Note 14), which
444 will be a valuable resource for the advancement of knowledge in the CPR research efforts.

445 Our effort to tackle the unknown provides a pathway to unlock a large pool of likely relevant data
446 that remains untapped to analysis and discovery. With the identification of a potential target gene
447 of unknown function for antibiotic resistance, we demonstrate the value of our approach and how
448 it can boost insights from model organism experiments. But severe challenges remain, such as
449 the dependence on the quality of the assemblies and their gene predictions, as shown by the
450 analysis of the ribosomal protein GCCs where many of the recovered genes are incomplete. While
451 sequence assembly has been an active area of research⁶⁰, this has not been the case for gene
452 prediction methods⁶⁰, which are becoming outdated⁶¹ and cannot cope with the current amount
453 of data. Alternatives like protein-level assembly⁶² combined with the exploration of the assembly
454 graphs' neighborhoods⁶³ become very attractive for our purposes. In any case, we still face the
455 challenge of discriminating between real and artifactual singletons⁶⁴. At the moment, there are no
456 methods available to provide a plausible solution and, at the same time, being scalable. We devise
457 a potential solution in the recent developments in unsupervised deep learning methods where
458 they use large corpora of proteins to define a language model *embedding* for protein sequences⁶⁵.
459 These models could be applied to predict *embeddings* in singletons, which could be clustered or
460 used to determine their coding potential. Another issue is that we might be creating more GCs
461 than expected. We follow a conservative approach to avoid mixing multidomain proteins in GCs
462 owing to the fragmented nature of the metagenome assemblies that could result in the split of a

463 GC. However, not only splitting can be a problem, but also lumping unrelated genes or GCs owing
464 to the use of remote homologies. Although the inference of GCCs is using very sensitive methods
465 to compare profile HMMs, low sequence diversity in GCs can limit its effectiveness. Our approach
466 is affected by the presence and propagation of contamination in reference databases, a significant
467 problem in 'omics^{66,67}. In our case, we only use Pfam as a source for annotation owing to its high-
468 quality and manual curation process. The categorization process of our GCs depends on the
469 information from other databases, and to minimize the potential impact of contamination, we apply
470 methods that weight the annotations of the identified homologs to discriminate if a GC belongs to
471 the known or unknown CDS-space. We foresee the integration of our approach to assist in the
472 manual curation process and increase the quality of the recovered MAGs⁶⁸.
473 The work presented here should incentivize the scientific community to build a collective effort to
474 define the different levels of unknown⁶⁹ where clear guidelines and protocols should be
475 established. Our work proves that the integration of the unknown fraction is possible and aims to
476 provide a new brighter future for microbiome analyses.
477

478 Material and methods

479 Genomic and metagenomic dataset

480 We used a set of 583 marine metagenomes from four of the major metagenomic surveys of the
481 ocean microbiome: Tara Oceans expedition (TARA)², Malaspina expedition⁷⁰, Ocean Sampling
482 Day (OSD)³, and Global Ocean Sampling Expedition (GOS)⁷¹. We complemented this set with
483 1,246 metagenomes obtained from the Human Microbiome Project (HMP) phase I and II⁷². We
484 used the assemblies provided by TARA, Malaspina, OSD and HMP projects and the long Sanger
485 reads from GOS⁷³. A total of 156M (156,422,969) contigs and 12.8M long-reads were collected
486 (Supp. Table 6).

487 For the genomic dataset, we used the 28,941 prokaryotic genomes (27,372 bacterial and 1,569
488 archaeal) from the Genome Taxonomy Database¹¹ (GTDB) Release 03-RS86 (19th August
489 2018).

490 Computational workflow development

491 We implemented a computation workflow based on Snakemake⁷⁴ for the easy processing of large
492 datasets in a reproducible manner. The workflow provides three different strategies to analyze

493 the data. The module *DB-creation* creates the gene cluster database, validates and partitions the
494 gene clusters (GCs) in the main functional categories. The module *DB-update* allows the
495 integration of new sequences (either at the contig or predicted gene level) in the existing gene
496 cluster database. In addition, the workflow has a *profile-search* function to quickly screen samples
497 using the gene cluster PSSM profiles in the database.

498 Metagenomic and genomic gene prediction

499 We used Prodigal (v2.6.3)⁷⁵ in metagenomic mode to predict the genes from the metagenomic
500 dataset. For the genomic dataset, we used the gene predictions provided by Annotree⁷⁶, since
501 they were obtained, consistently, with Prodigal v2.6.3. We identified potential spurious genes
502 using the *AntiFam* database⁷⁷. Furthermore, we screened for 'shadow' genes using the procedure
503 described in Yooseph et al.⁷⁸.

504 PFAM annotation

505 We annotated the predicted genes using the *hmmsearch* program from the *HMMER* package
506 (version: 3.1b2)⁷⁹ in combination with the Pfam database v31⁸⁰. We kept the matches exceeding
507 the internal gathering threshold and presenting an independent e-value < 1e-5 and coverage >
508 0.4. In addition, we took into account multi-domain annotations, and we removed overlapping
509 annotations when the overlap is larger than 50%, keeping the ones with the smaller e-value.

510 Determination of the gene clusters

511 We clustered the metagenomic predicted genes using the cascaded-clustering workflow of the
512 MMseqs2 software⁵⁷ ("*--cov-mode 0 -c 0.8 --min-seq-id 0.3*"). We discarded from downstream
513 analyses the singletons and clusters with a size below a threshold identified after applying a
514 broken-stick model⁸¹. We integrated the genomic data into the metagenomic cluster database
515 using the "DB-update" module of the workflow. This module uses the *clusterupdate* module of
516 MMseqs2³⁶, with the same parameters used for the metagenomic clustering.

517 Quality-screening of gene clusters

518 We examined the GCs to ensure their high intra-cluster homogeneity. We applied two
519 methodologies to validate their cluster sequence composition and functional annotation
520 homogeneity. We identified non-homologous sequences inside each cluster combining the

521 identification of a new cluster representative sequence via a sequence similarity network (SSN)
522 analysis, and the investigation of intra-cluster multiple sequence alignments (MSAs), given the
523 new representative. Initially, we generated an SSN for each cluster, using the semi-global
524 alignment methods implemented in *PARASAIL*⁸² (version 2.1.5). We trimmed the SSN using a
525 custom algorithm^{83,84} that removes edges while maintaining the network structural integrity and
526 obtaining the smallest connected graph formed by a single component. Finally, the new cluster
527 representative was identified as the most central node of the trimmed SSN by the eigenvector
528 centrality algorithm, as implemented in *igraph*⁸⁵. After this step, we built a multiple sequence
529 alignment for each cluster using *FAMSA*⁸⁶ (version 1.1). Then, we screened each cluster-MSA
530 for non-homologous sequences to the new cluster representative. Owing to computational
531 limitations, we used two different approaches to evaluate the cluster-MSAs. We used *LEON-BIS*⁸⁷
532 for the clusters with a size ranging from 10 to 1,000 genes and OD-SEQ⁸⁸ for the clusters with
533 more than 1,000 genes. In the end, we applied a broken-stick model⁸¹ to determine the threshold
534 to discard a cluster.

535 The predicted genes can have multi-domain annotations in different orders, therefore to validate
536 the consistency of intra-cluster Pfam annotations, we applied a combination of w-shingling⁸⁹ and
537 Jaccard similarity. We used w-shingling (k-shingle = 2) to group consecutive domain annotations
538 as a single object. We measured the homogeneity of the *shingle sets* (sets of domains) between
539 genes using the Jaccard similarity and reported the median similarity value for each cluster.
540 Moreover, we took into consideration the Clan membership of the Pfam domains and that a gene
541 might contain N-, C- and M-terminal domains for the functional homogeneity validation. We
542 discarded clusters with a median similarity < 1.

543 After the validation, we refined the gene cluster database removing the clusters identified to be
544 discarded and the clusters containing $\geq 30\%$ *shadow genes*. Lastly, we removed the single
545 shadow, spurious and non-homologous genes from the remaining clusters (Supplementary Note
546 2).

547 Remote homology classification of gene clusters

548 To partition the validated GCs into the four main categories, we processed the set of GCs
549 containing Pfam annotated genes and the set of not annotated GCs separately. For the annotated
550 GCs, we inferred a consensus protein domain architecture (DA) (an ordered combination of
551 protein domains) for each annotated gene cluster. To identify each gene cluster consensus DA,
552 we created directed acyclic graphs connecting the Pfam domains based on their topological order
553 on the genes using *igraph*⁸⁵. We collapsed the repetitions of the same domain. Then we used the

554 gene completeness as a positive-weighting value for the selection of the cluster consensus DA.
555 Within this step, we divided the GCs into "Knowns" (Known) if annotated to at least one Pfam
556 domains of known function (DKFs) and "Genomic unknowns" (GU) if annotated entirely to Pfam
557 domains of unknown function (DUFs).

558 We aligned the sequences of the non-annotated GCs with FAMSA⁸⁶ and obtained cluster
559 consensus sequences with the *hhconsensus* program from *HH-SUITE*³⁷. We used the cluster
560 consensus sequences to perform a nested search against the UniRef90 database (release
561 2017_11)⁹⁰ and NCBI *nr* database (release 2017_12)⁹¹ to retrieve non-Pfam annotations with
562 *MMSeqs2*³⁶ ("*-e 1e-05 --cov-mode 2 -c 0.6*"). We kept the hits within 60% of the Log(best-e-value)
563 and searched the annotations for any of the terms commonly used to define proteins of unknown
564 function (Supp. Table 12). We used a quorum majority voting approach to decide if a gene cluster
565 would be classified as *Genomic Unknown* or *Known without Pfams* based on the annotations
566 retrieved. We searched the consensus sequences without any homologs in the UniRef90
567 database against NCBI *nr*. We applied the same approach and criteria described for the first
568 search. Ultimately, we classified as *Environmental Unknown* those GCs whose consensus
569 sequences did not align with any of the NCBI *nr* entries.

570 In addition, we developed some conservative measures to control the trade-off between specificity
571 and sensitivity for the remote homology searches such as (1) a modification of the algorithm
572 described in Hingamp et al.⁹² to get a confident group of homologs to determine if a query protein
573 is known or unknown by a quorum majority voting approach (Supp Note 3); (2) strict parameters
574 in terms of iterations, bidirectional coverage and probability thresholds for the HHblits alignments
575 to minimize the inclusion of non-homologous sequences; and (3) avoid providing annotations for
576 our gene clusters, as we believe that annotation should be a careful process done on a smaller
577 scale and with experimental context.

578 Gene cluster remote homology refinement

579 We refined the *Environmental Unknown* GCs to ensure the lack of any characterization by
580 searching for remote homologies in the Uniclust database (release 30_2017_10) using the
581 HMM/HMM alignment method *HHblits*⁹³. We created the HMM profiles with the *hhmake* program
582 from the *HH-SUITE*³⁷. We only accepted those hits with an *HHblits-probability* $\geq 90\%$ and we re-
583 classified them following the same majority vote approach as previously described. The clusters
584 with no hits remained as the refined set of EUs. We applied a similar refinement approach to the
585 KWP clusters to identify GCs with remote homologies to Pfam protein domains. The KWP HMM
586 profiles were searched against the Pfam *HH-SUITE* database (version 31), using *HHblits*. We

587 accepted hits with a probability $\geq 90\%$ and a target coverage $> 60\%$ and removed overlapping
588 domains as described earlier. We moved the KWP with remote homologies to known Pfams to
589 the Known set, and those showing remote homologies to Pfam DUFs to the GUs. The clusters
590 with no hits remained as the refined set of KWP.

591 Gene cluster characterization

592 To retrieve the taxonomic composition of our clusters we applied the *MMseqs2 taxonomy* program
593 (version: b43de8b7559a3b45c8e5e9e02cb3023dd339231a), which allows computing the lowest
594 common ancestor through the implementation of the 2bLCA protocol⁹². We searched all cluster
595 genes against UniProtKB (release of January 2018)⁹⁴ using the following parameters “-e 1e-05 -
596 -cov-mode 0 -c 0.6”. We parsed the results to keep only the hits within 60% of the log10(best-e-
597 value). To retrieve the taxonomic lineages, we used the R package *CHNOSZ*⁹⁵. We measured
598 the intra-cluster taxonomic admixture by applying the *entropy.empirical()* function from the *entropy*
599 R package⁹⁶. This function estimates the Shannon entropy based on the different taxonomic
600 annotation frequencies. For each cluster, we also retrieved the cluster consensus taxonomic
601 annotation, which we defined as the taxonomic annotation of the majority of the genes in the
602 cluster.

603 In addition to the taxonomy, we evaluated the clusters' level of darkness and disorder using the
604 Dark Proteome Database (DPD)⁴⁰ as reference. We searched the cluster genes against the DPD,
605 applying the *MMseqs2* search program³⁶ with “-e 1e-20 --cov-mode 0 -c 0.6”. For each cluster,
606 we then retrieved the mean and the median level of darkness, based on the gene DPD
607 annotations.

608 High-quality clusters

609 We defined a subset of high-quality clusters based on the completeness of the cluster genes and
610 their representatives. We identified the minimum required percentage of complete genes per
611 cluster by a broken-stick model⁸¹ applied to the percentage distribution. Then, we selected the
612 GCs found above the threshold and with a complete representative.

613 A set of non-redundant domain architectures

614 We estimated the number of potential domain architectures present in the *Known* GCs taking into
615 account the large proportion of fragmented genes in the metagenomic dataset and that could
616 inflate the number of potential domain architectures. To identify fragments of larger domain

617 architecture, we took into account their topological order in the genes. To reduce the number of
618 comparisons, we calculated the pairwise string cosine distance (q-gram = 3) between domain
619 architectures and discarded the pairs that were too divergent (cosine distance ≥ 0.9). We
620 collapsed a fragmented domain architecture to the larger one when it contained less than 75% of
621 complete genes.

622 Inference of gene cluster communities

623 We aggregated distant homologous GCs into GCCs. The community inference approach
624 combined an all-vs-all HMM gene cluster comparison with Markov Cluster Algorithm (MCL)⁹⁷
625 community identification. We started performing the inference on the Known GCs to use the Pfam
626 DAs as constraints. We aligned the gene cluster HMMs using HHblits⁹³ (-n 2 -Z 10000000 -B
627 10000000 -e 1) and we built a homology graph using the cluster pairs with probability $\geq 50\%$ and
628 bidirectional coverage $> 60\%$. We used the ratio between HHblits-bitscore and aligned-columns
629 as the edge weights (Supp. Note 9). We used MCL⁹⁷ (v. 12-068) to identify the communities
630 present in the graph. We developed an iterative method to determine the optimal MCL inflation
631 parameter that tries to maximize the relationship of five intra-/inter-community properties: (1) the
632 proportion of MCL communities with one single DA, based on the consensus DAs of the cluster
633 members; (2) the ratio of MCL communities with more than one cluster; (3) the proportion of MCL
634 communities with a PFAM clan entropy equal to 0; (4) the intra-community HHblits-score/Aligned-
635 columns score (normalized by the maximum value); and (5) the number of MCL communities,
636 which should, in the end, reflect the number of non-redundant DAs. We iterated through values
637 ranging from 1.2 to 3.0, with incremental steps of 0.1. During the inference process, some of the
638 GCs became orphans in the graph. We applied a three-step approach to assigning a community
639 membership to these GCs. First, we used less stringent conditions (probability $\geq 50\%$ and
640 coverage $\geq 40\%$) to find homologs in the already existing GCCs. Then, we ran a second iteration
641 to find secondary relationships between the newly assigned GCs and the missing ones. Lastly,
642 we created new communities with the remaining GCs. We repeated the whole process with the
643 other categories (KWP, GU and EU), applying the optimal inflation value found for the Known (2.2
644 for metagenomic and 2.5 for genomic data).

645 Gene cluster communities validation

646 We tested the biological significance of the GCCs using the phylogeny of proteorhodopsin⁴⁴ (PR).
647 We used the proteorhodopsin HMM profiles⁴² to screen the marine metagenomic datasets using

648 *hmmsearch* (version 3.1b2)⁷⁹. We kept the hits with a coverage > 0.4 and e-value ≤ 1e-5. We
649 removed identical duplicates from the sequences assigned to PR with CD-HIT⁹⁸ (v4.6) and
650 cleaned from sequences with less than 100 amino acids. To place the identified PR sequences
651 into the MicRhode⁴⁴ PR tree first, we optimized the initial tree parameters and branch lengths with
652 RAxML (v8.2.12)⁹⁹. We used PaPaRA (v2.5)¹⁰⁰ to incrementally align the query PR sequences
653 against the MicRhode PR reference alignment and *pplacer*¹⁰¹ (v1.1.alpha19-0-g807f6f3) to place
654 the sequences into the tree. Finally, we assigned the query PR sequences to the MicRhode PR
655 Superclusters based on the phylogenetic placement. We further investigated the GCs annotated
656 as viral (196 genes, 14 GC) comparing them to the six newly discovered viral PRs¹⁰² using
657 Parasail⁸² (-a sg_stats_scan_sse2_128_16 -t 8 -c 1 -x). As an additional evaluation, we
658 investigated the distributions of standard GCCs and HQ GCCs within ribosomal protein families.
659 We obtained the ribosomal proteins used for the analysis combining the set of 16 ribosomal
660 proteins from Méheust et al.⁴³ and those contained in the collection of bacterial single-copy genes
661 of Anvi'o¹⁰³. Also, for the ribosomal proteins, we compared the outcome of our method to the one
662 proposed by Méheust et al.⁴³ (Supp. Note 9).

663 Metagenomic sample selection for downstream analyses

664 For the subsequent ecological analyses we selected those metagenomes with a number of genes
665 larger or equal to the first quartile of the distribution of all the metagenomic gene counts. (Supp.
666 Table 13).

667 Gene cluster abundance profiles in genomes and metagenomes

668 We estimated abundance profiles for the metagenomic cluster categories using the read coverage
669 to each predicted gene as a proxy for abundance. We calculated the coverage by mapping the
670 reads against the assembly contigs using the *bwa-mem* algorithm from *BWA mapper*¹⁰⁴. Then,
671 we used *BEDTOOLS*¹⁰⁵, to find the intersection of the gene coordinates to the assemblies, and
672 normalize the per-base coverage by the length of the gene. We calculated the cluster abundance
673 in a sample as the sum of the cluster gene abundances in that sample, and the cluster category
674 abundance in a sample as the sum of the cluster abundances. We obtained the proportions of
675 the different gene cluster categories applying a total-sum-scaling normalization. For the genomic
676 abundance profiles, we used the number of genes in the genomes and normalized by the total
677 gene counts per genome.

678 Rate of genomic and metagenomic gene clusters accumulation

679 We calculated the cumulative number of known and unknown GCs as a function of the number
680 of metagenomes and genomes. For each metagenome count, we generated 1000 random sets,
681 and we calculated the number of GCs and GCCs recovered. For this analysis, we used 1,246
682 HMP metagenomes and 358 marine metagenomes (242 from TARA and 116 from Malaspina).
683 We repeated the same procedure for the genomic dataset. We removed the singletons from the
684 metagenomic dataset with an abundance smaller than the mode abundance of the singletons that
685 got reclassified as good-quality clusters after integrating the GTDB data to minimize the impact
686 of potential spurious singletons. To complement those analyses, we evaluated the coverage of
687 our dataset by searching seven different state-of-the-art databases against our set of
688 metagenomic GC HMM profiles (Supp. Note 12).

689

690 Occurrence of gene clusters in the environment

691 We used 1,264 metagenomes from the TARA Oceans, MALASPINA Expedition, OSD2014 and
692 HMP-I/II to explore the properties of the unknown CDS-space in the environment. We applied the
693 Levins Niche Breadth (NB) index¹⁰⁶ to investigate the GCs and GCCs environmental distributions.
694 We removed the GCs and cluster communities with a mean relative abundance $< 1e-5$. We
695 followed a divide-and-conquer strategy to avoid the computational burden of generating the null-
696 models to test the significance of the distributions owing to the large number of metagenomes
697 and GCs. First, we grouped similar samples based on the gene cluster content using the Bray-
698 Curtis dissimilarity¹⁰⁷ in combination with the *Dynamic Tree Cut*¹⁰⁸ R package. We created 100
699 random datasets picking up one random sample from each group. For each of the 100 random
700 datasets, we created 100 random abundance matrices using the *nullmodel* function of the
701 *quasiswap* count method¹⁰⁹. Then we calculated the *observed* NB and obtained the 2.5% and
702 97.5% quantiles based on the randomized sets. We compared the observed and quantile values
703 for each gene cluster and defined it to have a *Narrow distribution* when the *observed* was smaller
704 than the 2.5% quantile and to have a *Broad distribution* when it was larger than the 97.5%
705 quantile. Otherwise, we classified the cluster as *Non-significant*¹¹⁰. We used a majority voting
706 approach to get a consensus distribution classification based on the ten random datasets.

707 Identification of prophages in genomic sequences

708 We used PhageBoost (<https://github.com/ku-cbd/PhageBoost/>) to find gene regions in the microbial
709 genomes that result in high viral signals against the overall genome signal. We set the following
710 thresholds to consider a region prophage: minimum of 10 genes, maximum 5 gaps, single-gene
711 probability threshold 0.9. We further smoothed the predictions using Parzen rolling windows of 20
712 periods and looked at the smoothed probability distribution across the genome. We disregarded
713 regions that had a summed smoothed probability less than 0.5, and those regions that did differ
714 from the overall population of the genes in a genome by using Kruskal–Wallis rank test (p-value
715 0.001).

716 Lineage-specific gene clusters

717 We used the F1-score developed for AnnoTree⁷⁶ to identify the lineage-specific GCs and to which
718 rank they are specific. Following similar criteria to the ones used in Mendler et al.⁷⁶, we considered
719 a gene cluster to be lineage-specific if it is present in less than half of all genomes and at least 2
720 with F1-score > 0.95.

721 Phylogenetic conservation of gene clusters

722 We calculated the phylogenetic conservation (τD) of each gene cluster using the *consenTRAIT*⁵⁰
723 function implemented in the R package *castor*⁵⁰. We used a paired Wilcoxon rank-sum test to
724 compare the average τD values for lineage-specific and non-specific GCs.

725 Evaluation of the OM-RGC v2 uncharacterized fraction

726 We integrated the 46,775,154 genes from the second version of the TARA Ocean Microbial
727 Reference Gene Catalog (OM-RGC v2)⁵³ into our cluster database using the same procedure as
728 for the genomic data. We evaluated the uncharacterized fraction and the genes classified into the
729 eggNOG⁵⁴ category S within the context of our database.

730 Augmenting experimental data

731 We searched the 37,684 genes of unknown function associated with mutant phenotypes from
732 Price et al.¹³ against our gene cluster profiles. We kept the hits with e-value $\leq 1e-20$ and a query
733 coverage > 60%. Then we filtered the results to keep the hits within 90% of the Log(best-e-value),
734 and we used a majority vote function to retrieve the consensus category for each hit. Lastly, we

735 selected the best-hits based on the smallest e-value and the largest query and target coverage
736 values. We used the fitness values from the RB-TnSeq experiments from Price et al. to identify
737 genes of unknown function that are important for fitness under certain experimental conditions.

738 Code and data availability

739 The code used for the analyses in the manuscript is available at [https://github.com/functional-](https://github.com/functional-dark-side/functional-dark-side.github.io/tree/master/scripts)
740 [dark-side/functional-dark-side.github.io/tree/master/scripts](https://github.com/functional-dark-side/functional-dark-side.github.io/tree/master/scripts). The code to recreate the figures is
741 available at https://github.com/functional-dark-side/vanni_et_al-figures. Detailed descriptions of
742 the different methods and results of this manuscript are available at
743 <https://dark.metagenomics.eu>. The workflow AGNOSTOS is available at
744 <https://github.com/functional-dark-side/agnostos-wf>, and its database can be downloaded from
745 <https://doi.org/10.6084/m9.figshare.12459056>.

746

747

748 Acknowledgments

749 The authors thankfully acknowledge the computer resources at MareNostrum and the technical
750 support provided by Barcelona Supercomputing Center (RES-AECT-2014-2-0085), the BMBF-
751 funded de.NBI Cloud within the German Network for Bioinformatics Infrastructure (de.NBI)
752 (031A537B, 031A533A, 031A538A, 031A533B, 031A535A, 031A537C, 031A534A, 031A532B),
753 the University of Oxford Advanced Research Computing
754 (<http://dx.doi.org/10.5281/zenodo.22558>) and the MARBITS bioinformatics core at ICM-CSIC. CV
755 was supported by the Max Planck Society. AFG received funding from the European Union's
756 Horizon 2020 research and innovation program Blue Growth: Unlocking the potential of Seas and
757 Oceans under grant agreement no. 634486 (project acronym INMARE). AM was supported by
758 the Biotechnology and Biological Sciences Research Council [BB/M011755/1, BB/R015228/1]
759 and RDF by the European Molecular Biology Laboratory core funds. EOC was supported by
760 project INTERACTOMA RTI2018-101205-B-I00 from the Spanish Agency of Science MICIU/AEI.
761 SGA and PS received additional funding by the project MAGGY (CTM2017-87736-R) from the
762 Spanish Ministry of Economy and Competitiveness. The Malaspina 2010 Expedition was
763 supported by the Spanish Ministry of Economy and Competitiveness (MINECO) through the

764 Consolidator-Ingenio program (ref. CSD2008-00077). The authors thank Johannes Söding and
765 Alex Bateman for helpful discussions.
766

767 Author Contributions

768 CV, MSS and AF-G performed the analyses and wrote the computational workflow. MS assisted
769 with the clustering and remote homology searches. KS helped with the identification of prophages
770 in genomic sequences. PLB and AB provided feedback and assisted with the ecological analyses.
771 RDF and AM provided feedback and information on the MGnify and Pfam databases. CMD, PS
772 and SGA provided the Malaspina metagenomes. TOD and AME analyzed data in the context of
773 metagenome-assembled genomes. AF-G conceived the study and supervised the work. CV and
774 AF-G wrote the manuscript. All authors read, edited and approved the final manuscript.
775
776

777 Competing Interests

778 The authors declare no competing interests.
779
780

781 References

- 782
- 783
- 784
- 785 1. Hug, L. A. *et al.* A new view of the tree of life. *Nat Microbiol* **1**, 16048 (2016).
- 786 2. Sunagawa, S. *et al.* Ocean plankton. Structure and function of the global ocean
- 787 microbiome. *Science* **348**, 1261359 (2015).
- 788 3. Kopf, A. *et al.* The ocean sampling day consortium. *Gigascience* **4**, 27 (2015).
- 789 4. Almeida, A. *et al.* A new genomic blueprint of the human gut microbiota. *Nature* **568**, 499–
- 790 504 (2019).
- 791 5. Pasolli, E. *et al.* Extensive Unexplored Human Microbiome Diversity Revealed by Over
- 792 150,000 Genomes from Metagenomes Spanning Age, Geography, and Lifestyle. *Cell* **176**,
- 793 649-662.e20 (2019).
- 794 6. Pachiadaki, M. G. *et al.* Charting the Complexity of the Marine Microbiome through Single-
- 795 Cell Genomics. *Cell* **179**, 1623-1635.e11 (2019).
- 796 7. Cross, K. L. *et al.* Targeted isolation and cultivation of uncultivated bacteria by reverse
- 797 genomics. *Nat. Biotechnol.* **37**, 1314–1321 (2019).
- 798 8. Eloë-Fadrosh, E. A. *et al.* Global metagenomic survey reveals a new bacterial candidate
- 799 phylum in geothermal springs. *Nat. Commun.* **7**, 10476 (2016).
- 800 9. Brown, C. T. *et al.* Unusual biology across a group comprising more than 15% of domain
- 801 Bacteria. *Nature* **523**, 208–211 (2015).
- 802 10. Spang, A. *et al.* Complex archaea that bridge the gap between prokaryotes and eukaryotes.
- 803 *Nature* **521**, 173–179 (2015).
- 804 11. Parks, D. H. *et al.* A standardized bacterial taxonomy based on genome phylogeny
- 805 substantially revises the tree of life. *Nat. Biotechnol.* **36**, 996–1004 (2018).
- 806 12. Bernard, G., Pathmanathan, J. S., Lannes, R., Lopez, P. & Bapteste, E. Microbial Dark
- 807 Matter Investigations: How Microbial Studies Transform Biological Knowledge and

- 808 Empirically Sketch a Logic of Scientific Discovery. *Genome Biol. Evol.* **10**, 707–715 (2018).
- 809 13. Price, M. N. *et al.* Mutant phenotypes for thousands of bacterial genes of unknown function.
810 *Nature* **557**, 503–509 (2018).
- 811 14. Carradec, Q. *et al.* A global ocean atlas of eukaryotic genes. *Nat. Commun.* **9**, 373 (2018).
- 812 15. Almeida, A. *et al.* A unified catalog of 204,938 reference genomes from the human gut
813 microbiome. *Nat. Biotechnol.* (2020) doi:10.1038/s41587-020-0603-3.
- 814 16. Mitchell, A. L. *et al.* MGnify: the microbiome analysis resource in 2020. *Nucleic Acids Res.*
815 **48**, D570–D578 (2020).
- 816 17. Quince, C., Walker, A. W., Simpson, J. T., Loman, N. J. & Segata, N. Shotgun
817 metagenomics, from sampling to analysis. *Nat. Biotechnol.* **35**, 833–844 (2017).
- 818 18. Franzosa, E. A. *et al.* Species-level functional profiling of metagenomes and
819 metatranscriptomes. *Nat. Methods* **15**, 962–968 (2018).
- 820 19. Huerta-Cepas, J. *et al.* Fast Genome-Wide Functional Annotation through Orthology
821 Assignment by eggNOG-Mapper. *Mol. Biol. Evol.* **34**, 2115–2122 (2017).
- 822 20. Chen, I.-M. A. *et al.* IMG/M v.5.0: an integrated data management and comparative
823 analysis system for microbial genomes and microbiomes. *Nucleic Acids Res.* **47**, D666–
824 D677 (2019).
- 825 21. Hanson, A. D., Pribat, A., Waller, J. C. & Crécy-Lagard, V. de. ‘Unknown’ proteins and
826 ‘orphan’ enzymes: the missing half of the engineering parts list--and how to find it. *Biochem.*
827 *J* **425**, 1–11 (2010).
- 828 22. Arnold, F. H. Design by Directed Evolution. *Acc. Chem. Res.* **31**, 125–131 (1998).
- 829 23. Brandenburg, O. F., Fasan, R. & Arnold, F. H. Exploiting and engineering hemoproteins for
830 abiological carbene and nitrene transfer reactions. *Curr. Opin. Biotechnol.* **47**, 102–111
831 (2017).
- 832 24. Arnold, F. H. Directed Evolution: Bringing New Chemistry to Life. *Angew. Chem. Int. Ed*
833 *Engl.* **57**, 4143–4148 (2018).

- 834 25. Jaroszewski, L. *et al.* Exploration of uncharted regions of the protein universe. *PLoS Biol.* **7**,
835 (2009).
- 836 26. Buttigieg, L. P. *et al.* Ecogenomic Perspectives on Domains of Unknown Function:
837 Correlation-Based Exploration of Marine Metagenomes. *PLoS One* **8**, (2013).
- 838 27. Yooseph, S. *et al.* The Sorcerer II global ocean sampling expedition: Expanding the
839 universe of protein families. *PLoS Biol.* **5**, 0432–0466 (2007).
- 840 28. Wyman, S. K., Avila-Herrera, A., Nayfach, S. & Pollard, K. S. A most wanted list of
841 conserved microbial protein families with no known domains. *PLoS One* **13**, e0205749
842 (2018).
- 843 29. Brum, J. R. *et al.* Illuminating structural proteins in viral “dark matter” with metaproteomics.
844 *Proc. Natl. Acad. Sci. U. S. A.* **113**, 2436–2441 (2016).
- 845 30. Bateman, A., Coghill, P. & Finn, D. R. DUFs: Families in search of function. *Acta*
846 *Crystallogr. Sect. F Struct. Biol. Cryst. Commun.* **66**, 1148–1152 (2010).
- 847 31. Lobb, B., Kurtz, D. A., Moreno-Hagelsieb, G. & Doxey, A. C. Remote homology and the
848 functions of metagenomic dark matter. *Front. Genet.* **6**, 1–12 (2015).
- 849 32. Bitard-Feildel, T. & Callebaut, I. Exploring the dark foldable proteome by considering
850 hydrophobic amino acids topology. *Sci. Rep.* **7**, 41425 (2017).
- 851 33. Bileschi, M. L. *et al.* Using Deep Learning to Annotate the Protein Universe. *bioRxiv* 626507
852 (2019) doi:10.1101/626507.
- 853 34. Liu, X. L. Deep Recurrent Neural Network for Protein Function Prediction from Sequence.
854 *bioRxiv* 103994 (2017) doi:10.1101/103994.
- 855 35. Rost, B. Twilight zone of protein sequence alignments. *Protein Eng. Des. Sel.* **12**, 85–94
856 (1999).
- 857 36. Steinegger, M. & Söding, J. MMseqs2 enables sensitive protein sequence searching for the
858 analysis of massive data sets. *Nat. Biotechnol.* **advance on**, (2017).
- 859 37. Steinegger, M. *et al.* HH-suite3 for fast remote homology detection and deep protein

- 860 annotation. *BMC Bioinformatics* **20**, 473 (2019).
- 861 38. Skewes-Cox, P., Sharpton, T. J., Pollard, K. S. & DeRisi, J. L. Profile hidden Markov
862 models for the detection of viruses within metagenomic sequence data. *PLoS One* **9**,
863 e105067 (2014).
- 864 39. Sberro, H. *et al.* Large-Scale Analyses of Human Microbiomes Reveal Thousands of Small,
865 Novel Genes. *Cell* **178**, 1245-1259.e14 (2019).
- 866 40. Perdigão, N., Rosa, A. C. & O'Donoghue, S. I. The Dark Proteome Database. *BioData Min.*
867 **10**, 1–11 (2017).
- 868 41. Habchi, J., Tompa, P., Longhi, S. & Uversky, V. N. Introducing protein intrinsic disorder.
869 *Chem. Rev.* **114**, 6561–6588 (2014).
- 870 42. Olson, D. K., Yoshizawa, S., Boeuf, D., Iwasaki, W. & DeLong, E. F. Proteorhodopsin
871 variability and distribution in the North Pacific Subtropical Gyre. *ISME J.* **12**, 1047–1060
872 (2018).
- 873 43. Méheust, R., Burstein, D., Castelle, C. J. & Banfield, J. F. The distinction of CPR bacteria
874 from other bacteria based on protein family content. *Nat. Commun.* **10**, 4173 (2019).
- 875 44. Boeuf, D., Audic, S., Brillet-Guéguen, L., Caron, C. & Jeanthon, C. MicRhoDE: a curated
876 database for the analysis of microbial rhodopsin diversity and evolution. *Database* **2015**,
877 (2015).
- 878 45. La Cono, V. *et al.* Partaking of Archaea to biogeochemical cycling in oxygen-deficient
879 zones of meromictic saline Lake Faro (Messina, Italy). *Environ. Microbiol.* **15**, 1717–1733
880 (2013).
- 881 46. Edwards, R. A. *et al.* Global phylogeography and ancient evolution of the widespread
882 human gut virus crAssphage. *Nat Microbiol* **4**, 1727–1736 (2019).
- 883 47. Dubinkina, V. B., Ischenko, D. S., Ulyantsev, V. I., Tyakht, A. V. & Alexeev, D. G.
884 Assessment of k-mer spectrum applicability for metagenomic dissimilarity analysis. *BMC*
885 *Bioinformatics* vol. 17 (2016).

- 886 48. Ma, Y. *et al.* Human papillomavirus community in healthy persons, defined by
887 metagenomics analysis of human microbiome project shotgun sequencing data sets. *J.*
888 *Virool.* **88**, 4786–4797 (2014).
- 889 49. Mendler, K. *et al.* AnnoTree: visualization and exploration of a functionally annotated
890 microbial tree of life. *Nucleic Acids Res.* **47**, 4442–4448 (2019).
- 891 50. Martiny, A. C., Treseder, K. & Pusch, G. Phylogenetic conservatism of functional traits in
892 microorganisms. *ISME J.* **7**, 830–838 (2013).
- 893 51. Rinke, C. *et al.* Insights into the phylogeny and coding potential of microbial dark matter.
894 *Nature* **499**, 431–437 (2013).
- 895 52. Anantharaman, K. *et al.* Expanded diversity of microbial groups that shape the dissimilatory
896 sulfur cycle. *ISME J.* **12**, 1715–1728 (2018).
- 897 53. Salazar, G. *et al.* Gene Expression Changes and Community Turnover Differentially Shape
898 the Global Ocean Metatranscriptome. *Cell* **179**, 1068-1083.e21 (2019).
- 899 54. Huerta-Cepas, J. *et al.* eggNOG 5.0: a hierarchical, functionally and phylogenetically
900 annotated orthology resource based on 5090 organisms and 2502 viruses. *Nucleic Acids*
901 *Res.* **47**, D309–D314 (2019).
- 902 55. Heffernan, B., Murphy, C. D. & Casey, E. Comparison of planktonic and biofilm cultures of
903 *Pseudomonas fluorescens* DSM 8341 cells grown on fluoroacetate. *Appl. Environ.*
904 *Microbiol.* **75**, 2899–2907 (2009).
- 905 56. Scales, B. S., Dickson, R. P., LiPuma, J. J. & Huffnagle, G. B. Microbiology, genomics, and
906 clinical significance of the *Pseudomonas fluorescens* species complex, an unappreciated
907 colonizer of humans. *Clin. Microbiol. Rev.* **27**, 927–948 (2014).
- 908 57. Steinegger, M. & Söding, J. Clustering huge protein sequence sets in linear time. *Nat.*
909 *Commun.* **9**, 2542 (2018).
- 910 58. Francino, M. P. The ecology of bacterial genes and the survival of the new. *Int. J. Evol.*
911 *Biol.* **2012**, 394026 (2012).

- 912 59. Muller, E. E. L. Determining Microbial Niche Breadth in the Environment for Better
913 Ecosystem Fate Predictions. *mSystems* **4**, (2019).
- 914 60. Roumpeka, D. D., Wallace, R. J., Escalettes, F., Fotheringham, I. & Watson, M. A Review
915 of Bioinformatics Tools for Bio-Prospecting from Metagenomic Sequence Data. *Front.*
916 *Genet.* **8**, 23 (2017).
- 917 61. Ivanova, N. N. *et al.* Stop codon reassignments in the wild. *Science* **344**, 909–913 (2014).
- 918 62. Steinegger, M., Mirdita, M. & Söding, J. Protein-level assembly increases protein sequence
919 recovery from metagenomic samples manyfold. *Nat. Methods* **16**, 603–606 (2019).
- 920 63. Titus Brown, C. *et al.* Exploring neighborhoods in large metagenome assembly graphs
921 reveals hidden sequence diversity. *bioRxiv* 462788 (2018) doi:10.1101/462788.
- 922 64. Höps, W., Jeffries, M. & Bateman, A. Gene Unprediction with Spurio: A tool to identify
923 spurious protein sequences. *F1000Res.* **7**, 261 (2018).
- 924 65. Heinzinger, M. *et al.* Modeling aspects of the language of life through transfer-learning
925 protein sequences. *BMC Bioinformatics* **20**, 723 (2019).
- 926 66. Breitwieser, F. P., Pertea, M., Zimin, A. & Salzberg, S. L. Human contamination in bacterial
927 genomes has created thousands of spurious proteins. *Genome Res.* (2019)
928 doi:10.1101/gr.245373.118.
- 929 67. Steinegger, M. & Salzberg, S. L. Terminating contamination: large-scale search identifies
930 more than 2,000,000 contaminated entries in GenBank. *Genome Biol.* **21**, 115 (2020).
- 931 68. Chen, L.-X., Anantharaman, K., Shaiber, A., Eren, A. M. & Banfield, J. F. Accurate and
932 complete genomes from metagenomes. *Genome Res.* **30**, 315–333 (2020).
- 933 69. Thomas, A. M. & Segata, N. Multiple levels of the unknown in microbiome research. *BMC*
934 *Biol.* **17**, 48 (2019).
- 935 70. Duarte, C. M. Seafaring in the 21st Century: The Malaspina 2010 Circumnavigation
936 Expedition. *Limnol. Oceanog. Bull.* **24**, 11–14 (2015).
- 937 71. Rusch, D. B. *et al.* The Sorcerer II Global Ocean Sampling Expedition: Northwest Atlantic

- 938 through Eastern Tropical Pacific. *PLoS Biol.* **5**, 1–34 (2007).
- 939 72. Lloyd-Price, J. *et al.* Strains, functions and dynamics in the expanded Human Microbiome
940 Project. *Nature* **550**, 61–66 (2017).
- 941 73. Sanger, F., Nicklen, S. & Coulson, A. R. DNA sequencing with chain-terminating inhibitors.
942 *Proc. Natl. Acad. Sci. U. S. A.* **74**, 5463–5467 (1977).
- 943 74. Köster, J. Reproducible data analysis with Snakemake. *F1000Res.* **7**, (2018).
- 944 75. Hyatt, D. *et al.* Prodigal: prokaryotic gene recognition and translation initiation site
945 identification. *BMC Bioinformatics* **11**, 119–119 (2010).
- 946 76. Mandler, K. *et al.* AnnoTree: visualization and exploration of a functionally annotated
947 microbial tree of life. *Nucleic Acids Res.* **47**, 4442–4448 (2019).
- 948 77. Eberhardt, R. Y. *et al.* AntiFam: a tool to help identify spurious ORFs in protein annotation.
949 *Database* **2012**, bas003–bas003 (2012).
- 950 78. Yooseph, S., Li, W. & Sutton, G. Gene identification and protein classification in microbial
951 metagenomic sequence data via incremental clustering. *BMC Bioinformatics* **9**, 1–13
952 (2008).
- 953 79. Finn, R. D., Clements, J. & Eddy, S. R. HMMER web server: interactive sequence similarity
954 searching. *Nucleic Acids Res.* **39**, W29–W37 (2011).
- 955 80. Finn, R. D. *et al.* The Pfam protein families database: towards a more sustainable future.
956 *Nucleic Acids Res.* **44**, D279–D285 (2016).
- 957 81. Bennett, K. D. Determination of the number of zones in a biostratigraphical sequence. *New*
958 *Phytol.* **132**, 155–170 (1996).
- 959 82. Daily, J. Parasail: SIMD C library for global, semi-global, and local pairwise sequence
960 alignments. *BMC Bioinformatics* **17**, 81–81 (2016).
- 961 83. Žure, M., Fernandez-Guerra, A., Munn, C. B. & Harder, J. Geographic distribution at
962 subspecies resolution level: closely related *Rhodopirellula* species in European coastal
963 sediments. *ISME J.* **11**, 478–489 (2017).

- 964 84. Chafee, M. *et al.* Recurrent patterns of microdiversity in a temperate coastal marine
965 environment. *ISME J.* **12**, 237–252 (2018).
- 966 85. Csardi, G. & Nepusz, T. The igraph software package for complex network research.
967 *InterJournal* vol. Complex Systems 1695 (2006).
- 968 86. Deorowicz, S., Debudaj-Grabysz, A. & Gudyś, A. FAMSA: Fast and accurate multiple
969 sequence alignment of huge protein families. *Sci. Rep.* **6**, 33964–33964 (2016).
- 970 87. Vanhoutreve, R. *et al.* LEON-BIS: multiple alignment evaluation of sequence neighbours
971 using a Bayesian inference system. *BMC Bioinformatics* **17**, 271–271 (2016).
- 972 88. Jehl, P., Sievers, F. & Higgins, D. G. OD-seq: outlier detection in multiple sequence
973 alignments. *BMC Bioinformatics* **16**, 269–269 (2015).
- 974 89. Broder, A. Z. On the resemblance and containment of documents. in *Proceedings.*
975 *Compression and Complexity of SEQUENCES 1997 (Cat. No. 97TB100171)* 21–29 (IEEE,
976 1997).
- 977 90. The UniProt Consortium. UniProt: the universal protein knowledgebase. *Nucleic Acids Res.*
978 **45**, D158–D169 (2017).
- 979 91. NCBI Resource Coordinators. Database resources of the National Center for Biotechnology
980 Information. *Nucleic Acids Res.* **46**, D8–D13 (2018).
- 981 92. Hingamp, P. *et al.* Exploring nucleo-cytoplasmic large DNA viruses in Tara Oceans
982 microbial metagenomes. *ISME J.* **7**, 1678–1695 (2013).
- 983 93. Remmert, M., Biegert, A., Hauser, A. & Söding, J. HHblits: Lightning-fast iterative protein
984 sequence searching by HMM-HMM alignment. *Nat. Methods* **9**, 173–175 (2012).
- 985 94. UniProt Consortium, T. UniProt: the universal protein knowledgebase. *Nucleic Acids Res.*
986 **46**, 2699 (2018).
- 987 95. Dick, J. M. Calculation of the relative metastabilities of proteins using the CHNOSZ
988 software package. *Geochem. Trans.* **9**, 10 (2008).
- 989 96. Hausser, J. & Strimmer, K. Entropy inference and the James-Stein estimator, with

- 990 application to nonlinear gene association networks. *arXiv [stat.ML]* (2008).
- 991 97. van Dongen, S. & Abreu-Goodger, C. Using MCL to Extract Clusters from Networks. in
992 *Bacterial Molecular Networks: Methods and Protocols* (eds. van Helden, J., Toussaint, A. &
993 Thieffry, D.) 281–295 (Springer New York, 2012).
- 994 98. Li, W. & Godzik, A. Cd-hit: a fast program for clustering and comparing large sets of protein
995 or nucleotide sequences. *Bioinformatics* **22**, 1658–1659 (2006).
- 996 99. Stamatakis, A. RAxML version 8: a tool for phylogenetic analysis and post-analysis of large
997 phylogenies. *Bioinformatics* **30**, 1312–1313 (2014).
- 998 100. Berger, S. A. & Stamatakis, A. PaPaRa 2.0: a vectorized algorithm for probabilistic
999 phylogeny-aware alignment extension. *Heidelberg Institute for Theoretical Studies*,
1000 <http://sco.h-its.org/exelixis/publications.html>. *Exelixis-RRDR-2012-2015* (2012).
- 1001 101. Matsen, F. A., Kodner, R. B. & Armbrust, E. V. pplacer: linear time maximum-likelihood and
1002 Bayesian phylogenetic placement of sequences onto a fixed reference tree. *BMC*
1003 *Bioinformatics* **11**, 538 (2010).
- 1004 102. Needham, D. M. *et al.* A distinct lineage of giant viruses brings a rhodopsin photosystem to
1005 unicellular marine predators. *Proc. Natl. Acad. Sci. U. S. A.* **116**, 20574–20583 (2019).
- 1006 103. Murat Eren, A. *et al.* Anvi'o: an advanced analysis and visualization platform for 'omics
1007 data. *PeerJ* **3**, e1319 (2015).
- 1008 104. Li, H. & Durbin, R. Fast and accurate long-read alignment with Burrows–Wheeler transform.
1009 *Bioinformatics* **26**, 589–595 (2010).
- 1010 105. Quinlan, A. R. & Hall, I. M. BEDTools: a flexible suite of utilities for comparing genomic
1011 features. *Bioinformatics* **26**, 841–842 (2010).
- 1012 106. Levins, R. THE STRATEGY OF MODEL BUILDING IN POPULATION BIOLOGY. *Am. Sci.*
1013 **54**, 421–431 (1966).
- 1014 107. Bray, J. R., Roger Bray, J. & Curtis, J. T. An Ordination of the Upland Forest Communities
1015 of Southern Wisconsin. *Ecological Monographs* vol. 27 325–349 (1957).

- 1016 108.Langfelder, P., Zhang, B. & Horvath, S. Defining clusters from a hierarchical cluster tree:
1017 the Dynamic Tree Cut package for R. *Bioinformatics* **24**, 719–720 (2008).
- 1018 109.Miklós, I. & Podani, J. RANDOMIZATION OF PRESENCE–ABSENCE MATRICES:
1019 COMMENTS AND NEW ALGORITHMS. *Ecology* vol. 85 86–92 (2004).
- 1020 110.Salazar, G. *et al.* Particle-association lifestyle is a phylogenetically conserved trait in
1021 bathypelagic prokaryotes. *Mol. Ecol.* **24**, 5692–5706 (2015).